An algorithm for estimating the generalized fundamental traffic variables from point measurements using initial conditions

Jamshidnejad, A.; De Schutter, B.

Important note
To cite this publication, please use the final published version (if applicable).
Please check the document version above.

Taylor & Francis
Taylor & Francis Group

An algorithm for estimating the generalized fundamental traffic variables from point measurements using initial conditions

A. Jamshidnejad and B. De Schutter

Delft Center for Systems and Control, Delft University of Technology, Delft, The Netherlands

ABSTRACT

Fundamental macroscopic traffic variables (flow, density, and average speed) have been defined in two ways: classical (defined as either temporal or spatial averages) and generalized (defined as temporal-spatial averages). In the available literature, estimation of the generalized variables is still missing. This paper proposes a new efficient sequential algorithm for estimating the generalized traffic variables using point measurements. The algorithm takes into account those vehicles that stay between two consecutive measurement points for more than one sampling cycle and that are not detected during these sampling cycles. The algorithm is introduced for single-lane roads first, and is extended to multi-lane roads. For evaluation of the proposed approach, Next Generation SIMulation (NGSIM) data, which provides detailed information on trajectories of the vehicles on a segment of the interstate freeway I-80 in San Francisco, California is used. The simulation results illustrate the excellent performance of the sequential procedure compared with other approaches.

1. Contributions and organization of the paper

Generalized traffic variables (Edie 1963) play an important role in traffic theory and applications. However, the available literature mostly focus on estimation of the traffic variables in their classical definition. To the best of our knowledge, except for the work by Jamshidnejad and De Schutter (2015), there is no papers on estimation of the generalized average speed from point measurements. This becomes more significant when one takes into account the extensive use of the inductive loop detectors worldwide (Klein, Mills, and Gibson 2006; Bickel et al. 2007), and the high costs of substituting them with new technologies. The main contributions of this paper include the following topics:

(1) We propose a new efficient method for estimation of the generalized fundamental traffic variables from point measurements. The proposed approach is suitable especially for cases where there is missing, disrupted, or limited information about the vehicles between two consecutive measurement points.

(2) We propose two methods to deal with the missing or disrupted information between two measurement points. For the two methods, vehicles between two consecutive measurement points follow two paradigms: constant speed and non-constant speed. The non-constant speed case is inspired by the approach proposed by Coifman (2002), but we have changed the method so that

CONTACT A. Jamshidnejad ✉ a.jamshidnejad@tudelft.nl 🖃 Delft Center for Systems and Control, Delft University of Technology, Mekelweg 2, 2628CD Delft, The Netherlands

it does not need the future information of a leading vehicle to produce the approximate trajectory of the following vehicle at the current time instant. Therefore, our approach can also be used for estimation of the trajectory of vehicles between two consecutive measurement points in real time.

(3) We develop a new sequential algorithm that takes into account the vehicles that might stay on the same sampling road section and between the same two consecutive measurement points during a number of sampling cycles. Hence, these vehicles are not detected at the measurement time instant. The proposed algorithm keeps track of the detected vehicles from the time instant they are observed at one measurement point, until they reach the next measurement point. Hence, compared with previous work that does not take these vehicles into account, our new approach can produce more accurate results.

(4) We show via real-life Next Generation SIMulation (NGSIM) data (captured on a segment of the interstate freeway I-80 in San Francisco, California, USA) that the proposed approach produces more accurate results compared with the available approaches.

The rest of the paper is organized as follows. In Section 2.1 we give an overview of the concepts used in this paper, and in Section 2.2 we discuss the previous work on estimation of the fundamental traffic variables from point measurements. In Section 3 we explain how the problem can be formulated in the time–space plane by defining the concept of sampling windows. Section 4 introduces the new
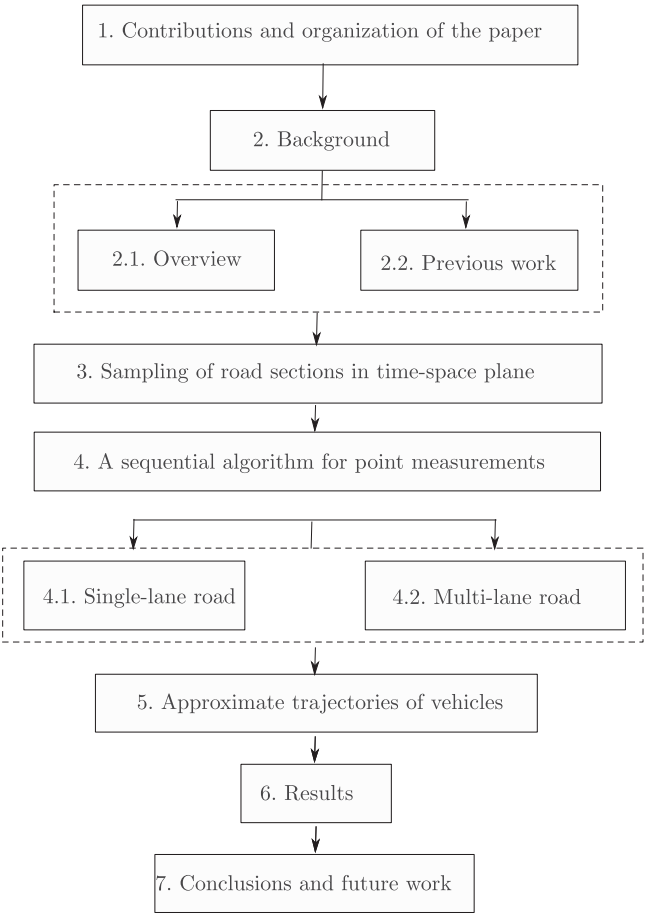

Figure 1. Road map of the paper.

Table 1. Mathematical notations used in the paper.

A	Area of a sampling region
n_A	Total number of trajectories observed in the sampling region of area A
t_0	Initial time instant
t^{end}	Final time instant
n_t	Total number of trajectories observed on a stretch of the road at time t
T_j	Sampling time for loop detector D_j
n_j^{cyc}	Number of (whole) sampling cycles occurring within $[t_0, t^{end}]$
i	Time step counter
$w_{i,j}$	Time–space sampling window corresponding to road section j considered at step i
$N_{G,i,j}$	Number of vehicles from group G in the sampling window $w_{i,j}$
$G_{G,i,j}$	Set of indices of the vehicles from group G in the sampling window $w_{i,j}$
ρ_A	Generalized density corresponding to sampling area A
q_A	Generalized flow corresponding to sampling area A
$\bar{v}_A$	Generalized average speed corresponding to sampling area A
$\rho_{i,j}$	Generalized density corresponding to sampling window $w_{i,j}$
$q_{i,j}$	Generalized flow corresponding to sampling window $w_{i,j}$
$\bar{v}_{i,j}$	Generalized average speed corresponding to sampling window $w_{i,j}$
$A_{i,j}$	Area of window $w_{i,j}$
$\theta_{c,i,j}$	Time instant, at which vehicle c is detected in $w_{i,j}$ by the inductive loop detector D_j
$L_{n^{loop}}^{endpoint}$	Distance between the last loop detector and the endpoint of the road
Δt_c^G	Total travel time of vehicle c from group G moving on a single-lane road
$s_c^{start,G}$	Initial relative position w.r.t. upstream loop detector of vehicle c from group G on a single-lane road
$s_c^{end,G}$	Final relative position w.r.t. upstream loop detector of vehicle c from group G on a single-lane road
d_c^G	Traveled distance of vehicle c from group G moving on a single-lane road
$\Delta t_{c,\ell}^G$	Total travel time of vehicle c from group G moving on lane ℓ
$s_{c,\ell}^{start,G}$	Initial relative position w.r.t. upstream loop detector of vehicle c from group G moving on lane ℓ
$s_{c,\ell}^{end,G}$	Final relative position w.r.t. upstream loop detector of vehicle c from group G moving on lane ℓ
$d_{c,\ell}^G$	Traveled distance of vehicle c from group G moving on lane ℓ

sequential algorithm that keeps track of the vehicles that are detected by inductive double-loop detectors, and produces the generalized density, flow, and average speed of vehicles. In Section 4.1, first the algorithm is developed for single-lane roads; and next, in Section 4.2, the algorithm is extended to multi-lane roads. Section 5 explains how to find approximate trajectories of the vehicles that are traveling on a sampling road section in between of two successive loop detectors. In Section 6, we present the results of a case study using NGSIM data in order to assess the efficiency of the proposed algorithm compared with formulas available in the literature. Finally, the paper is concluded in Section 7 and suggestions for future work are proposed. A road map of the paper is illustrated in Figure 1. In addition to that, Table 1 presents the mathematical notations that are used through the paper.

2. Background

2.1. Overview

Macroscopic fundamental traffic variables (density, flow, and average speed) are important in theory, analysis, control, and performance measurement of traffic (e.g. see Messner and Papageorgiou 1990; Daganzo 1995; Kamijo et al. 2000; Sheu 2002; Lee, Hellinga, and Saccomanno 2006; Wang, Papageorgiou, and Messmer 2006). These variables have been defined and formulated in two different ways:
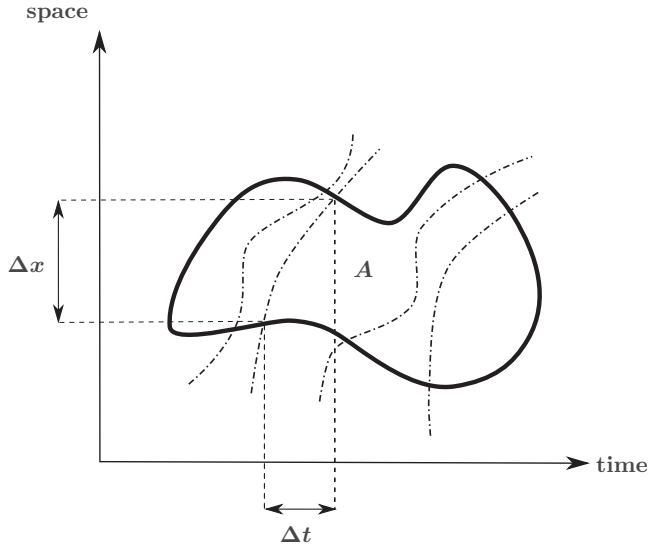
Figure 2. An arbitrary region in the time–space plane for defining the generalized fundamental traffic variables.

classical and generalized. In the classical definition (see Daganzo 1997 for detailed definitions), within the time–space plane, density is a spatial average, flow is a temporal average, and average speed is the ratio of flow and density (Wardrop 1952; Edie 1963; Daganzo 1997).

Edie (1963) proposes a more general definition for the fundamental traffic variables. Consider an arbitrarily shaped region of area A in the time–space plane (see Figure 2). Suppose that the dashed-dotted curves in Figure 2 illustrate the trajectories of some vehicles, with n_A the number of these vehicles. The generalized density, flow, and average speed within region A are given by

$$\rho_A = \frac{1}{A} \sum_{i=1}^{n_A} \Delta t_i, \quad q_A = \frac{1}{A} \sum_{i=1}^{n_A} \Delta x_i, \tag{1}$$

$$\bar{v}_A = \frac{q_A}{\rho_A}. \tag{2}$$

Our focus in this paper is to propose an approach for estimating the generalized traffic variables from point measurements.

2.2. Previous work

Several papers exist on estimation of the classical average speed, called the space-mean speed, from point measurements. To the best of our knowledge, there is no method currently available for estimating the generalized fundamental traffic variables from point measurements, except for the work by Jamshidnejad and De Schutter (2015). In this section, we briefly explain previous work on estimation of the average speed.

Rakha and Zhang (2005) prove the formula introduced by Khisty and Lall (2003) for estimating the space-mean speed v_s, which is given by

$$v_s \approx v_t - \frac{\sigma_t^2}{v_t}, \tag{3}$$

where v_t is the time-mean speed (see Daganzo 1997 for the definition), and σ_t is the temporal standard deviation of the individual speeds of the observed vehicles. Soriguera and Robusté (2011)

propose a formula to compute σ_t, where they assume a normal distribution for the speeds of the vehicles

$$\sigma_t = \frac{v^* - v_t}{\phi^{-1}\left(\frac{n_{v^*}}{n}\right)}, \tag{4}$$

with v^* a particular speed threshold, $\phi(\cdot)$ the cumulative distribution function of the standard normal distribution, n_{v^*} the number of observed vehicles moving with v^*, and n the total number of observed vehicles.

Wardrop ([1952]) proposes an equation for estimating the time-mean speed from a known space-mean speed, i.e.

$$v_t = v_s + \frac{\sigma_s^2}{v_s}, \tag{5}$$

with σ_s the spatial standard deviation of the observed speeds. As reported by Jamshidnejad and De Schutter ([2015]), Equation (5) may produce complex values for v_s. Han et al. ([2010]) suggest a different representation of Equation (5) that does not involve σ_s, but adds the mean value of the individual speed values:

$$v_s = 0.75v_t + 0.25\sqrt{9v_t^2 - 8E[v_i^2]}, \tag{6}$$

where $E(\cdot)$ denotes the expected value, and v_i is the observed speed of the vehicle i.

Estimation of the generalized average speed $\bar{v}_A$ is considered by Jamshidnejad and De Schutter ([2015]), where tight upper and lower bounds for $\bar{v}_A$ are given by

$$\bar{v}^{\text{low}} = \frac{n - 0.5\,m + 0.5}{n - m + 1 + \frac{0.5m(m-1)}{M-1}} H_{n-m+1}, \tag{7}$$

$$\bar{v}^{\text{up}} = \frac{n - 0.5M + 1}{n - m + 1 + \frac{0.5(M-1)(2m-M)}{m}} H_{n-m+1}, \tag{8}$$

in which

$$m = \left\lfloor \frac{L}{hv_{\min}} \right\rfloor + 1, \quad M = \left\lfloor \frac{L}{hv_{\max}} \right\rfloor + 1, \tag{9}$$

with L the distance between two consecutive measurement points, h the average time headway of the observed vehicles, $v_{\min}$ and $v_{\max}$ the minimum and maximum of the speeds, and H_{n-m+1} the harmonic mean of the speeds of the first $n-m+1$ observed vehicles. Finally, Jamshidnejad and De Schutter ([2015]) introduce a convex combination of the proposed bounds to estimate $\bar{v}$, i.e.

$$\bar{v} = \frac{\bar{v}^{\text{up}} + \gamma \bar{v}^{\text{low}}}{1 + \gamma}, \quad \gamma \geq 0, \tag{10}$$

where γ is either identified using an extensive dataset, or is computed as $\gamma = v_{\max}/v_{\min}$.

In this paper, we propose a new method to estimate the generalized fundamental traffic variables from point measurements. We first assume constant speeds for the vehicles, and later we propose an approach for approximating the trajectories of the vehicles in the time–space plane, which is inspired by Coifman ([2002]).

Coifman ([2002]) proposes a method to estimate trajectories of vehicles between two consecutive double-loop detectors based on available point measurements. According to Lighthill and Whitham ([1955]), if a change in speed occurs at a point of a certain traffic stream, this change will back-propagate through the traffic stream with a fixed speed. The speed of the back-propagation of the change depends on the governing traffic situation (free-flow or congested). Coifman ([2002]) applies
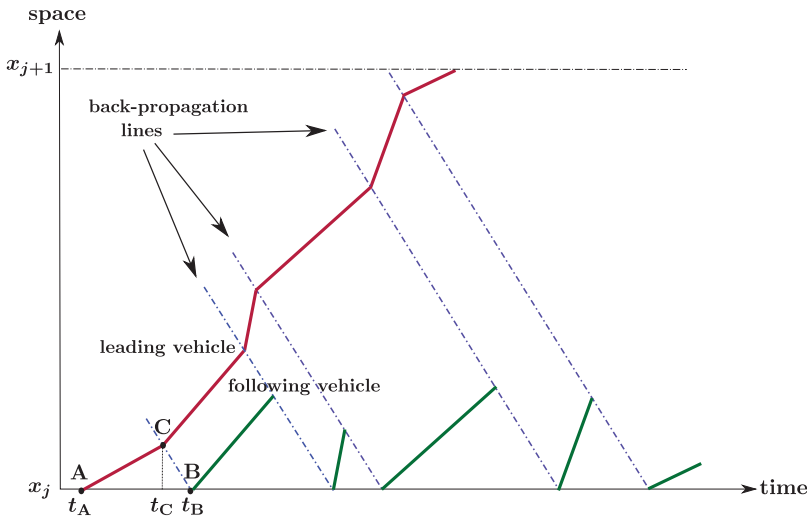
Figure 3. Estimating the trajectories of vehicles based on the approach proposed by Coifman (2002).

this result to find the approximate trajectories. Suppose that speed measurements of two successive vehicles are available at points 'A' and 'B' within the time–space plane (see Figure 3), with these points located at the loop detector line and corresponding to time instants t_A and t_B.

Coifman (2002) plots the back-propagation lines (see the blue dashed-dotted lines in Figure 3) with a fixed slope equal to the back-propagation speed. These back-propagation lines originate at points in the time–space plane, where speed measurements are available (e.g. at point 'B' in Figure 3). As soon as a vehicle's trajectory intersects with one of these back-propagation lines, it changes its slope to one of the trajectory of the leading vehicle (e.g. at point 'C' in Figure 3, the trajectory changes its slope to the slope of the trajectory of the vehicle observed at point 'B').

This actually means that the vehicle observed at point 'B' has been following the vehicle observed at point 'A', and at point 'B', this vehicle adapts its speed to the speed of the leading vehicle at point 'C'. In practice, since the speed measurements are available only at the loop detector line (i.e. at location x_j in Figure 3, the slope of the trajectory of the leading vehicle at point 'C' can be extracted from the slope of the trajectory of the following vehicle at point 'B'. This is not a problem for off-line processing of the dataset of course, but this approach cannot be implemented on-line.

Note that the approach proposed by Coifman (2002) is based on the Newell's car-following model and on the assumption that the adapting point of the following vehicle, i.e. the point in the time–space plane at which the following vehicle changes its speed to that of the leading vehicle, is located at the loop detector line.

Inspired by the approach given by Coifman (2002), in Section 5, we will propose a new method for estimating the trajectory of the leading vehicle without any need to capture measurements from the following vehicle at some time ahead (e.g. measurements from t_B in Figure 3 for instant t_C which occurs before t_B). We propose a model for movement of the main leading vehicle of a traffic stream that is based on the assumption that the leading vehicle intends to reach the free-flow speed as soon as possible. Then, we just need to know the initial speed of the leading vehicle in a sampling cycle to approximate its trajectory, where this initial speed is either measured at a measurement point, or is announced by the proposed sequential algorithm in case the leading vehicle is between two consecutive measurement points at the beginning of the sampling time. The trajectories of the following vehicles are then found using Newell's car-following model. Hence, trajectory of a leading vehicle is extracted independent from that of the following vehicle, and this makes our proposed methodology suitable for on-line applications.

3. Sampling of road sections in the time–space plane

In this section, we first represent and define the problem introducing the concept of a sampling road section, and its illustration in the time–space plane. Since our focus is on computation of the generalized fundamental traffic variables, we first need to map the problem into the time–space plane. Note that the main mathematical notations used in this paper are listed in Table 1.

Consider a road of length L^{road}, with n^{loop} inductive loop detectors represented by D_j installed at positions $x_j, j \in \{1, 2, \ldots, n^{loop}\}$, where L_j, i.e. the distance between any two consecutive loop detectors D_j and D_{j+1}, is represented by

$$L_j = x_{j+1} - x_j. \tag{11}$$

Hence,

$$L_{n^{loop}}^{endpoint} = x^{endpoint} - x_{n^{loop}}.$$

Note that to define the positions and distances on a road, we first consider a virtual curve that can be plotted across the middle points of the road's width, i.e. the centerline of the road, and its shape follows the shape of the road (see the dashed curve in Figure 4(a)). Then we consider an equivalent straight road, for which the length is equal to the length of the centerline curve (see Figure 4(b)). The traffic conditions on the road will be investigated for a total time period $[t_0, t^{end}]$ of length T^{road} using data from inductive loop detectors.

To present and process traffic data, trajectories of vehicles can be plotted in the time–space plane (Treiber and Kesting 2013), where the processing time is shown on the horizontal axis, and the processed length of the road is shown on the vertical axis (see Figure 5). We first consider a single-lane
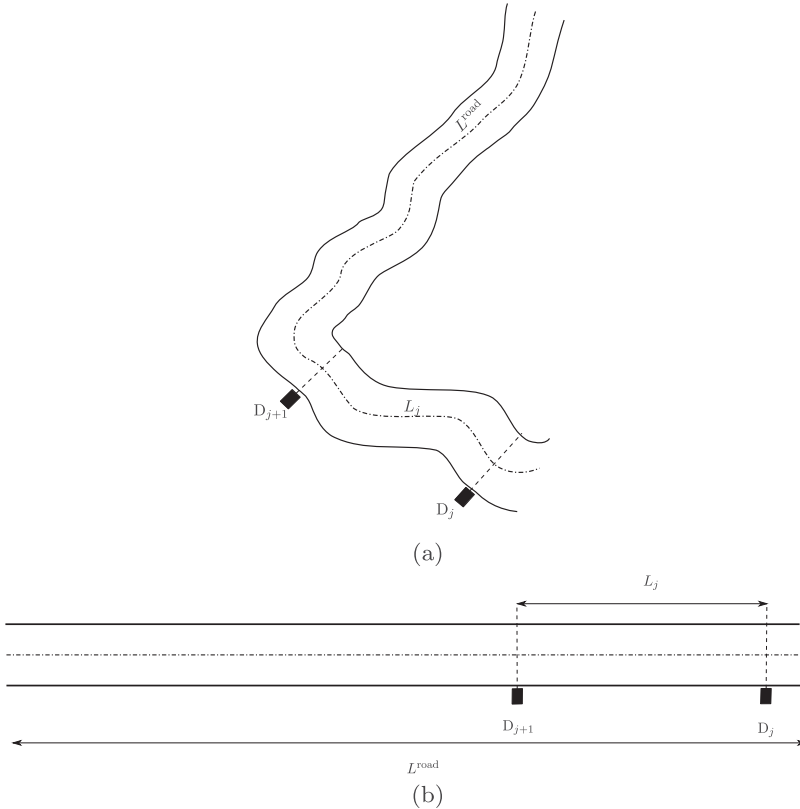

Figure 4. Mapping the real road into Cartesian coordinates. (a) Real shape of the road and (b) equivalent road.

road, where the space axis is directed through the direction of movement. The representation of the road in the time–space plane will be a rectangular frame of length L^{road} and of width T^{road} (see the main frame in Figure 5). Suppose that we want to find the fundamental traffic variables at time step t_i (i.e. for the time period between steps $t_{i-1,j}$ and $t_{i,j}$) on a piece of the road that is extended between two successive loop detectors D_j and D_{j+1}. The piece of the road of length L_j with D_j and D_{j+1} as its upstream and downstream loop detectors ($j \in \{1, 2, \ldots, n^{\text{loop}}\}$) is called a *sampling road section*, which is indexed by the index j; the representation of the sampling road section j in the time–space plane is a window of length L_j and of width T_j, which is called a *sampling window*, indexed by the time step counter i and by the index of the upstream loop detector j. Figure 5 illustrates the time–space sampling windows with a length of L_j and a width of T_j, with $j \in \{1, \ldots, n^{\text{loop}}\}$. For each sampling window, the lower edge is located along the line $x = x_j$, i.e. at the position of the upstream inductive loop detector, of the corresponding sampling road section.

For a sampling window $w_{i,j}$, with $i \in \{1, 2, \ldots, n_j^{\text{cyc}}\}$ and $j \in \{1, 2, \ldots, n^{\text{loop}}\}$, the right, left, top, and bottom edges of the sampling window are denoted by, respectively, $\text{E}|_{i,j}$, $|\text{E}_{i,j}$, $\bar{\text{E}}_{i,j}$, and $\underline{\text{E}}_{i,j}$ (see Figure 5). The trajectories of those vehicles that are observed by the upstream loop detector during the current sampling cycle will intersect the lower edge $\underline{\text{E}}_{i,j}$ of the sampling window.

Now, it should be checked if any of the trajectories according to those vehicles that will be observed within the area of $w_{i,j}$ might enter $w_{i,j}$ via the left edge of the window, $|\text{E}_{i,j}$; vehicles corresponding to these trajectories will spend some time in $w_{i,j}$ and, therefore, will affect the average speed and the average density of this sampling window. However, since they will not pass through the detection zone of the upstream loop detector at $x = x_j$ in the current cycle, they will not be detected. Therefore, we should keep track of them from the previous cycle(s), and then use their information, including their speed and location at $t_{i-1,j}$ as the initial conditions for the current cycle time.

The main question here is whether we need to check all previous windows $w_{\ell,m}$, for $\ell = 1, 2, \ldots, i - 1$ and $m = 1, 2, \ldots, j$ to process $w_{i,j}$, or whether it is possible to reduce the effort. Considering the rectangles in the same row of the grid shown in Figure 5 (e.g. the grey windows for processing $w_{i,j}$) will be sufficient, because the trajectories of all vehicles that enter $w_{i,j}$ and have previously traveled in the
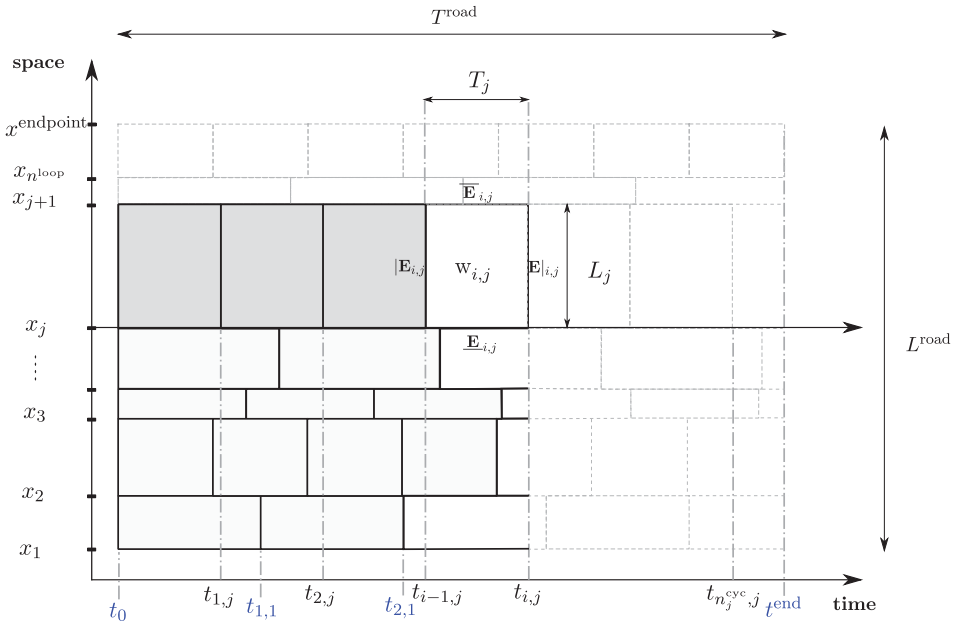

Figure 5. The time–space plot for the sampling road sections on a road of length L^{road} being processed during a total time of T^{road} using data from inductive loop detectors.

sampling windows located in lower rows of the grid (i.e. with $x_m < x_j$), should definitely cross the line $x = x_j$ before they enter $w_{i,j}$ and hence they will once be observed by loop detector D_j. However, the vehicles that are located at position x_c at $t_{i,j}$ with $x_j < x_c < x_{j+1}$, i.e. vehicles that were (partly) traveling in the same road section during the previous cycle, will not be detected by the upstream loop detector. To keep track of these vehicles, we should consider the sampling window located in the left-hand side of $w_{i,j}$ in the same row, i.e. $w_{i-1,j}$ (see Figure 5); and similarly for $w_{i-1,j}$ we should keep track of the information in $w_{i-2,j}$, and so on. Consequently, we consider separate time indicators $t_{i,j}$, $i \in \{1, \ldots, n_j^{cyc}\}$ for each row of the sampling windows in Figure 5.

Note that in this paper we define four groups of vehicles for every sampling window $w_{i,j}$; $G_{1,i,j}$, $G_{2,i,j}$, $G_{3,i,j}$, and $G_{4,i,j}$ referring to, respectively, the group of vehicles that enter the sampling road section j during cycle i, the group of vehicles that are already in the sampling road section j at the beginning of cycle i, the group of vehicles that leave the sampling road section by the end of cycle i, and the group of vehicles that will stay on the sampling road section at the end of cycle i.

4. A sequential algorithm for point measurements to keep track of all vehicles

4.1. Single-lane roads

All discussions presented in this section are based on the following assumptions:

Assumption 4.1: The first loop detector on the processed road is located at the beginning point of the road.

Assumption 4.2: The road is considered to have only a single lane (this assumption will later on be relaxed in Section 4.2).

Assumption 4.3: All vehicles travel with a constant speed (reported by the upstream loop detector) on each sampling road section, until a new speed value is detected for them by the downstream loop detector (this assumption will be relaxed later on in Section 5).

For the work presented in this paper, the assumption of stationary traffic conditions is not required.

Figure 6(a) illustrates three sampling windows $w_{i-1,j}$, $w_{i,j}$, and $w_{i+1,j}$ in the time–space plane that represent sampling road section j during three successive sampling cycles of length T_j starting at $t_{i-2,j}$, $t_{i-1,j}$, and $t_{i,j}$. Figure 6(b) illustrates $w_{i,j}$ and different groups of vehicles that are observed in this window. The indices of those vehicles, for which the trajectories pass through $\underline{E}_{i,j}$ are stored in $G_{1,i,j}$, and the indices of those vehicles, for which the trajectories intersect $|E_{i,j}$ are stored in $G2, i, j$. From Figure 6(a), for any vehicle $c_1 \in \{1, 2, \ldots, N_{1,i,j}\}$ in $w_{i,j}$ we obtain:

Case 1. If $s_{c_1}^{end,G_{1,i,j}}$, then the vehicle leaves $w_{i,j}$ through its upper edge and will not enter $w_{i+1,j}$; indices of those vehicles in $G_{1,i,j}$ that satisfy this condition are stored in subgroup $G_{1,i,j}^{(1)}$ of $G_{1,i,j}$;

Case 2. If $s_{c_1}^{end,G_{1,i,j}} < L_j$, then the vehicle leaves $w_{i,j}$ through its right-hand edge, and enters $w_{i+1,j}$ through its left-hand edge; indices of those vehicles that satisfy this condition are stored in subgroup $G_{1,i,j}^{(2)}$ of $G_{1,i,j}$;

Similarly, for any vehicle $c_2 \in \{1, 2, \ldots, N_{2,i,j}\}$ in $w_{i,j}$ we obtain:

Case 3. If $s_{c_2}^{end,G_{2,i,j}} \geq L_j$, then the vehicle leaves $w_{i,j}$ through its upper edge and will not enter $w_{i+1,j}$; indices of those vehicles in $G_{2,i,j}$ that satisfy this condition are stored in subgroup $G_{2,i,j}^{(1)}$ of $G_{2,i,j}$;

Case 4. If $s_{c_2}^{end,G_{2,i,j}} < L_j$, then the vehicle leaves $w_{i,j}$ through its right-hand edge, and enters $w_{i+1,j}$ through its left-hand edge; indices of those vehicles that satisfy this condition are stored in subgroup $G_{2,i,j}^{(2)}$ of $G_{2,i,j}$.

Therefore, $G_{1,i,j}^{(1)}$ and $G_{2,i,j}^{(1)}$ will form $G_{1,i,j+1}$, and will not play any role in the sampling window $w_{i+1,j}$, while $G_{1,i,j}^{(2)}$ and $G_{2,i,j}^{(2)}$ will form $G_{2,i+1,j}$.
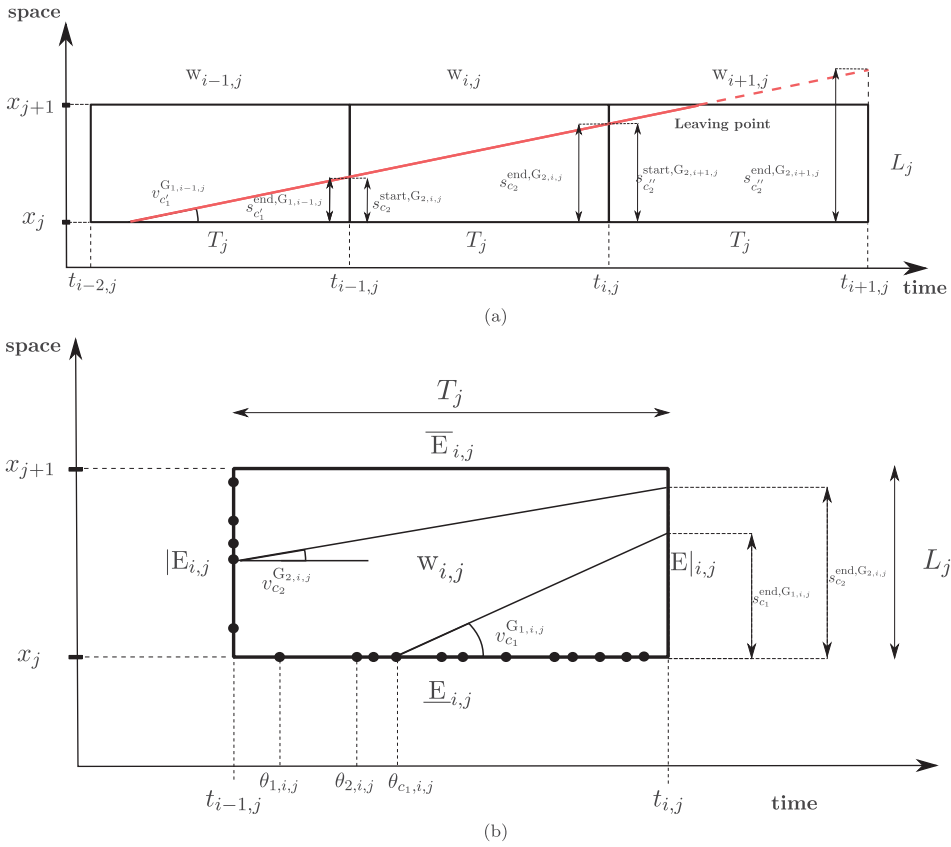
Figure 6. Sampling windows corresponding to the same road section during successive sampling cycles. (a) Successive sampling cycles. (b) Sampling window $w_{i,j}$ and different groups of vehicles observed.

From Figure 6(b), the total travel time of a vehicle $c_1 \in \{1, \ldots, N_{1,i,j}\}$ from $G_{1,i,j}$ within one cycle time is obtained as

$$\Delta t_{c_1}^{G_{1,i,j}} = T_j + t_{i-1,j} - \theta_{c_1,i,j}. \tag{12}$$

The total traveled distance by any vehicle c_1 during one sampling cycle equals:

$$d_{c_1}^{G_{1,i,j}} = v_{c_1}^{G_{1,i,j}} \cdot \Delta t_{c_1}^{G_{1,i,j}}, \tag{13}$$

and for the relative position of c_1 at $t = t_{i-1,j}$ and at $t = t_{i,j}$ w.r.t. $x = x_j$, we have

$$s_{c_1}^{\text{start}, G_{1,i,j}} = 0, \tag{14}$$

$$s_{c_1}^{\text{end}, G_{1,i,j}} = d_{c_1}^{G_{1,i,j}}. \tag{15}$$

The total travel time of a vehicle $c_2 \in \{1, 2, \ldots, N_{2,i,j}\}$ from $G_{2,i,j}$ during one sampling cycle is

$$\Delta t_{c_2}^{G_{2,i,j}} = T_j. \tag{16}$$

The total distance traveled by any vehicle c_2 during one sampling cycle is computed by

$$d_{c_2}^{G_{2,i,j}} = v_{c_2}^{G_{2,i,j}} \Delta t_{c_2}^{G_{2,i,j}}, \tag{17}$$

in which

$$v_{c_2}^{G2,i,j} = v_{c_g'}^{G_g,i-1,j},$$ (18)

where c_g' denotes the index of the given vehicle in $w_{i-1,j}$, supposing that it belonged to group $G_{g,i-1,j}, g \in \{1, 2\}$ while in $w_{i-1,j}$. Hence the start and the end positions are :[1]

$$s_{c_2}^{\text{start},G2,i,j} = s_{c_g'}^{\text{end},G_g,i-1,j},$$ (19)

$$s_{c_2}^{\text{end},G2,i,j} = d_{c_2}^{G2,i,j} + s_{c_2}^{\text{start},G2,i,j}.$$ (20)

The new procedure sequentially uses Equations (12)–(20), and computes the generalized average speed, the generalized flow, and the generalized density using the following equations

$$\rho_{i,j} = \frac{1}{A_{i,j}} \sum_{g=1}^{2} \sum_{c_g \in G_{g,i,j}} \min \left\{ \Delta t_{c_g}^{G_g,i,j}, \frac{L_j - s_{c_g}^{\text{start},G_g,i,j}}{v_{c_g}^{G_g,i,j}} \right\},$$ (21)

$$q_{i,j} = \frac{1}{A_{i,j}} \sum_{g=1}^{2} \sum_{c_g \in G_{g,i,j}} \min \left\{ d_{c_g}^{G_g,i,j}, L_j - s_{c_g}^{\text{start},G_g,i,j} \right\},$$ (22)

$$\bar{v}_{i,j} = \frac{\rho_{i,j}}{q_{i,j}}.$$ (23)

Algorithm 1 represents the sequential algorithm proposed for a single-lane road. The total number of operations that the sequential algorithm involves can be determined as follows; suppose that for a specific loop detector, within one sampling cycle, n vehicles are observed in total. Then, from Algorithm 1, the total number of multiplications is $3(n + 1)$ and the total number of summations is less than $3.5n$, where the total number of summations depends on the number of vehicles that are in either of groups 1 and 2 introduced in Section 3 of the paper. Note that $3.5n$ is the maximum possible number of the summations and is reached for the case where there are the same number of vehicles in groups 1 and 2.

4.2. Multi-lane roads

In the previous section, we considered a single-lane road (see Assumption 4.2 of Section 4.1). Here we will relax this assumption by considering a multi-lane road and by extending the sequential procedure to a multi-lane road case (in order to avoid making the derived equations too complicated by involving a lane-changing model, here we assume that there are no lane changes).

Suppose that the road has N^{lane} lanes; we consider the sampling road section j that is extended between two consecutive loop detectors D_j and D_{j+1}. Suppose that during $[t_{i-1,j}, t_{i,j}]$, $N_{1,i,j}$ vehicles have entered the sampling road section (through all N^{lane} lanes) at time instants $\theta_{1,i,j}, \theta_{2,i,j}, \ldots, \theta_{N_{1,i,j},i,j}$, where the values of $\theta_{c_1,i,j}$ for $c_1 \in \{1, \ldots, N_{1,i,j}\}$ are not necessarily distinct, i.e. it is possible to have two vehicles entering the sampling road section j at the same time instant via different lanes. Define $v_{c_1,\ell}^{G1,i,j}$ as the speed of the vehicle that enters the sampling road section j at time instant $\theta_{c_1,i,j}, c_1 \in \{1, \ldots, N_{1,i,j}\}$ through lane $\ell, \ell \in \{1, \ldots, N^{\text{lane}}\}$.

Now we can represent each lane of the sampling road section in the time–space plane by a sampling window $w_{i,j}^\ell$, which indicates the sampling window corresponding to the ℓth lane of the sampling road section j. Figure 7 illustrates such sampling windows. Note that we consider the set $\mathcal{D}_{i,j}$ as the set of distinct time instants in the time–space plane for all sampling windows $w_{i,j}^\ell$. Suppose that $\mathcal{D}_{i,j}$ has

---

Algorithm 1 Computation of fundamental traffic variables on a single-lane road for the jth loop detector, $j \in \{1, 2, \ldots, n^{\text{loop}}\}$

1: **Input:** $\begin{cases} L^{\text{road}}, T^{\text{road}}, L_j, T_j \\ v_{c_1}^{G_{1,i,j}}, \theta_{c_1,i,j}, t_{i-1,j} \quad \forall c_1 \in \{1, \ldots, N_{1,i,j}\}, \forall i \in \{1 \ldots, n_j^{\text{cyc}}\}, n_j^{\text{cyc}} = \left\lfloor \frac{T^{\text{road}}}{T_j} \right\rfloor \\ v_{c_2}^{G_{2,0,j}} \qquad\qquad \forall c_2 \in \{1, \ldots, N_{2,0,j}\} \end{cases}$

2: **Output:** $\rho_{i,j}, q_{i,j}, \bar{v}_{i,j}$

3: **for** $i = 1$ to n_j^{cyc} **do**

4:      **for** $c_1 = 1$ to $N_{1,i,j}$ **do**

5:          compute $\Delta t_{c_1}^{G_{1,i,j}}$ from (12),
6:          compute $d_{c_1}^{G_{1,i,j}}$ from (13),
7:          compute $s_{c_1}^{\text{end},G_{1,i,j}}$ from (15),
8:          use **Case 1** and **Case 2** to construct $G_{1,i,j}^{(1)}$ and $G_{1,i,j}^{(2)}$,
9:          $v_{c_2''}^{G_{2,i+1,j}} \leftarrow v_{c_1}^{G_{1,i,j}}$ where $\{c_2''$ is the index of vehicle c_1 in $G_{2,i+1,j}\}$

10:      **end for**

11:      **for** $c_2 = 1$ to $N_{2,i,j}$ **do**

12:          compute $\Delta t_{c_2}^{G_{2,i,j}}$ from (16),
13:          compute $d_{c_2}^{G_{2,i,j}}$ from (17),
14:          compute $s_{c_2}^{\text{end},G_{2,i,j}}$ from (20),
15:          use **Case 3** and **C4** to construct $G_{2,i,j}^{(1)}$ and $G_{2,i,j}^{(2)}$,
16:          $v_{c_2''}^{G_{2,i+1,j}} \leftarrow v_{c_2}^{G_{2,i,j}}$,   where $\{c_2''$ is the index of vehicle c_2 in $G_{2,i+1,j}\}$
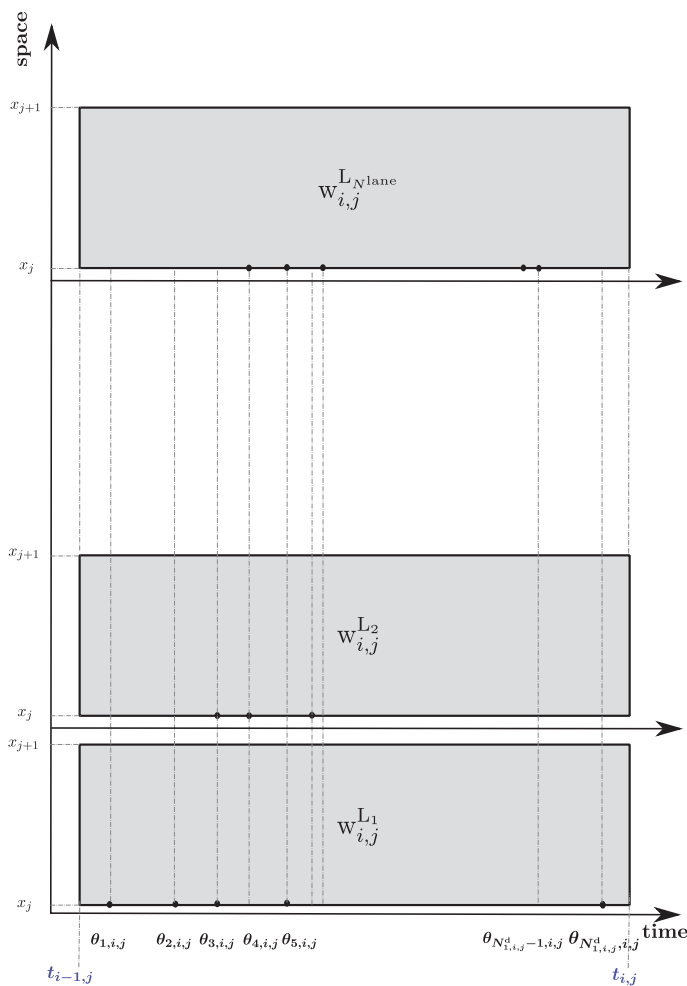17: $s_{c_2''}^{\text{start},G_{2,i+1,j}} \leftarrow s_{c_2}^{\text{end},G_{2,i,j}}$

18:      **end for**

19:      $G_{2,i+1,j} \leftarrow G_{1,i,j}^{(2)} \bigcup G_{2,i,j}^{(2)}$

20:      compute $\rho_{i,j}$ from (21),
21:      compute $q_{i,j}$ from (22),
22:      compute $\bar{v}_{i,j}$ from (23)

23: **end for**

Figure 7. Time–space plots for a multi-lane road.

$N^{\mathrm{d}}_{1,i,j}$ members ($N^{\mathrm{d}}_{1,i,j} \leq N_{1,i,j}$). Then $v^{G_{1,ij}}_{c_1,\ell}$ for $c_1 \in \{1, \ldots, N^{\mathrm{d}}_{1,ij}\}$ will be substituted by either the observed speed on lane ℓ at time instant $\theta_{c_1,i,j}$, or by zero if no vehicles have been observed (i.e. we consider a virtual vehicle with zero speed in this case). This way we can summarize all the data corresponding to

the sampling road section in a matrix of dimension $N^{\text{lane}} \times N^{\text{d}}_{1,i,j}$ (see also Figure 7)

$$V^{G_{1,i,j}} = \begin{bmatrix} v^{G_{1,i,j}}_{1,1} & v^{G_{1,i,j}}_{2,1} & v^{G_{1,i,j}}_{3,1} & 0 & \cdots & 0 & v^{G_{1,i,j}}_{N^{\text{d}}_{1,i,j},1} \\ 0 & 0 & v^{G_{1,i,j}}_{3,2} & v^{G_{1,i,j}}_{4,2} & \cdots & 0 & 0 \\ \vdots & \vdots & \vdots & \vdots & \cdots & \vdots & \vdots \\ \vdots & \vdots & \vdots & \vdots & \cdots & \vdots & \vdots \\ 0 & 0 & 0 & v^{G_{1,i,j}}_{4,N^{\text{lane}}} & \cdots & v^{G_{1,i,j}}_{N^{\text{d}}_{1,i,j}-1,N^{\text{lane}}} & 0 \end{bmatrix}. \tag{24}$$

The parameters $\theta_{1,i,j}$, $\theta_{2,i,j}$, $\ldots$ $\theta_{N^{\text{d}}_{1,i,j},i,j}$ are the time instants, at which each of the vehicles (real or virtual) is positioned at x_j. We use an $N^{\text{d}}_{1,i,j} \times N^{\text{d}}_{1,i,j}$ matrix defined as

$$\Theta^{G_{1,i,j}} = \begin{bmatrix} \theta_{1,i,j} & 0 & 0 & \cdots & 0 \\ 0 & \theta_{2,i,j} & 0 & \cdots & 0 \\ \vdots & \vdots & \vdots & \cdots & \vdots \\ \vdots & \vdots & \vdots & \cdots & \vdots \\ 0 & 0 & 0 & \cdots & \theta_{N^{\text{d}}_{1,i,j},i,j} \end{bmatrix}. \tag{25}$$

We have

$$\Delta t^{G_{1,i,j}}_{c_1,\ell} = (T_j + t_{i-1,j} - \theta_{c_1,i,j}) \cdot \text{sign}(v^{G_{1,i,j}}_{c_1,\ell}), \tag{26}$$

$$d^{G_{1,i,j}}_{c_1,\ell} = v^{G_{1,i,j}}_{c_1,\ell} \cdot \Delta t^{G_{1,i,j}}_{c_1,\ell}, \tag{27}$$

$$s^{\text{start},G_{1,i,j}}_{c_1,\ell} = 0, \tag{28}$$

$$s^{\text{end},G_{1,i,j}}_{c_1,\ell} = d^{G_{1,i,j}}_{c_1,\ell}, \tag{29}$$

where $i \in \{1, \ldots, n^{\text{cyc}}_j\}$, $j \in \{1, \ldots, n^{\text{loop}}\}$, $c_1 \in \{1, \ldots, N^{\text{d}}_{1,i,j}\}$, and $\ell \in \{1, \ldots, N^{\text{lane}}\}$. Finally, we obtain the following equation for all vehicles in $G_{1,i,j}$:

$$\Delta T^{G_{1,i,j}} = \text{sign}(V^{G_{1,i,j}}) \cdot ((T_j + t_{i-1,j}) \cdot I_{N^{\text{d}}_{1,i,j} \times N^{\text{d}}_{1,i,j}} - \Theta^{G_{1,i,j}}), \tag{30}$$

$$D^{G_{1,i,j}} = V^{G_{1,i,j}} \cdot ((T_j + t_{i-1,j}) \cdot I_{N^{\text{d}}_{1,i,j} \times N^{\text{d}}_{1,i,j}} - \Theta^{G_{1,i,j}}), \tag{31}$$

$$S^{\text{start},G_{1,i,j}} = 0, \tag{32}$$

$$S^{\text{end},G_{1,i,j}} = D^{G_{1,i,j}}, \tag{33}$$

where $\text{sign}(\cdot)$ operates element-wise on a matrix, and produces a matrix with the same dimension as the input matrix, i.e.

$$\text{sign}([a_{kl}]_{N \times N}) = [\text{sign}(a_{kl})]_{N \times N}$$

and $\Delta T^{G_{1,i,j}}$, $D^{G_{1,i,j}}$, $S^{\text{start},G_{1,i,j}}$, and $S^{\text{end},G_{1,i,j}}$ are matrices of dimension $N^{\text{lane}} \times N^{\text{d}}_{1,i,j}$.

For the second group of vehicles ($G_{2,i,j}$) that have entered the sampling road section within previous cycles, and that are therefore located at the left-hand side of the sampling windows, $V^{G_{2,i,j}}$ will again

be a matrix of the following form:

$$
V^{G_{2,i,j}} = \begin{bmatrix}
v_{1,1}^{G_{2,i,j}} & v_{2,1}^{G_{2,i,j}} & v_{3,1}^{G_{2,i,j}} & \cdots & v_{N_{2,i,j}^{d},1}^{G_{2,i,j}} \\
v_{1,2}^{G_{2,i,j}} & v_{2,2}^{G_{2,i,j}} & v_{3,2}^{G_{2,i,j}} & \cdots & v_{N_{2,i,j}^{d},2}^{G_{2,i,j}} \\
\vdots & \vdots & \vdots & \vdots & \cdots & \vdots & \vdots \\
v_{1,N^{\text{lane}}}^{G_{2,i,j}} & v_{2,N^{\text{lane}}}^{G_{2,i,j}} & v_{3,N^{\text{lane}}}^{G_{2,i,j}} & \cdots & v_{N_{2,i,j}^{d},N^{\text{lane}}}^{G_{2,i,j}}
\end{bmatrix},
\tag{34}
$$

which is of dimension $N^{\text{lane}} \times N_{2,i,j}^{d}$, with $N_{2,i,j}^{d} = \max\{N_{2,i,j}^{\ell}\}$ where $N_{2,i,j}^{\ell}$ shows the number of vehicles in $G_{2,i,j}$ that are traveling on lane ℓ. For lanes with $N_{2,i,j}^{\ell} < N_{2,i,j}^{d}$, the corresponding elements of $V^{G_{2,i,j}}$ on columns $N_{2,i,j}^{\ell} + 1$ are set to zero. We obtain

$$
\Delta t_{c_2,\ell}^{G_{2,i,j}} = T_j \cdot \text{sign}(v_{c_2,\ell}^{G_{2,i,j}}),
\tag{35}
$$

$$
d_{c_2,\ell}^{G_{2,i,j}} = v_{c_2,\ell}^{G_{2,i,j}} \Delta t_{c_2,\ell}^{G_{2,i,j}},
\tag{36}
$$

$$
s_{c_2,\ell}^{\text{start},G_{2,i,j}} = s_{c_g',\ell}^{\text{end},G_{g,i-1,j}},
\tag{37}
$$

$$
s_{c_2,\ell}^{\text{end},G_{2,i,j}} = d_{c_2,\ell}^{G_{2,i,j}} + s_{c_2,\ell}^{\text{start},G_{2,i,j}},
\tag{38}
$$

where g is the group to which vehicle c_2 belonged in $w_{i-1,j}$ and c_g' is the index of this vehicle in $G_{g,i-1,j}$. Hence,

$$
\Delta T^{G_{2,i,j}} = \text{sign}(V^{G_{2,i,j}})T_j,
\tag{39}
$$

$$
D^{G_{2,i,j}} = T_j V^{G_{2,i,j}},
\tag{40}
$$

$$
S^{\text{start},G_{2,i,j}} = S^{\text{end},G_{g,i-1,j}},
\tag{41}
$$

$$
S^{\text{end},G_{2,i,j}} = D^{G_{2,i,j}} + S^{\text{start},G_{2,i,j}},
\tag{42}
$$

with $\Delta T^{G_{2,i,j}}$, $D^{G_{2,i,j}}$, $S^{\text{start},G_{2,i,j}}$, and $S^{\text{end},G_{2,i,j}}$ matrices of dimension $N^{\text{lane}} \times N_{2,i,j}^{d}$, and $S^{\text{end},G_{g,i-1,j}}$ a matrix, which has as its (c,ℓ)th element, $s_{c,\ell}^{\text{end},G_{g,i-1,j}}$ corresponding to the vehicle with speed $v_{c,\ell}^{G_{2,i,j}}$ (where g is again the group to which this vehicle belonged in $w_{i-1,j}$).

In order to find the generalized density, flow, and average speed for each lane separately, we can write

$$
\rho_{i,j}^{\ell} = \frac{1}{A_{i,j}} \sum_{g=1}^{2} \sum_{c=1}^{N_{g,i,j}^{d}} \min\left\{ \Delta T_{\ell,c}^{G_{g,i,j}}, \frac{L_j - S_{\ell,c}^{\text{start},G_{g,i,j}}}{V_{\ell,c}^{G_{g,i,j}}} \right\},
\tag{43}
$$

$$
q_{i,j}^{\ell} = \frac{1}{A_{i,j}} \sum_{g=1}^{2} \sum_{c=1}^{N_{g,i,j}^{d}} \min\{D_{\ell,c}^{G_{g,i,j}}, L_j - S_{\ell,c}^{\text{start},G_{g,i,j}}\},
\tag{44}
$$

$$
\bar{v}_{i,j}^{\ell} = \frac{\rho_{i,j}^{\ell}}{q_{i,j}^{\ell}},
\tag{45}
$$

and to find the generalized traffic variables for the lane altogether, we have

$$\rho_{i,j} = \frac{1}{N^{\text{lane}} A_{i,j}} \sum_{\ell=1}^{N^{\text{lane}}} \rho_{i,j}^{\ell}, \tag{46}$$

$$q_{i,j} = \frac{1}{N^{\text{lane}} A_{i,j}} \sum_{\ell=1}^{N^{\text{lane}}} q_{i,j}^{\ell}, \tag{47}$$

$$\bar{v}_{i,j} = \frac{\rho_{i,j}}{q_{i,j}}. \tag{48}$$

Algorithm 1 can easily be extended for the multi-lane road using the introduced matrices.

5. Approximate trajectories of vehicles based on Newell's car-following model

In the previous sections, we have considered that each vehicle will move with a constant speed in $w_{i,j}$ (see Assumption 4.3 of Section 4.1), i.e. for $c_1 \in \{1, \dots, N_{1,i,j}\}$ and for $c_2 \in \{1, \dots, N_{2,i,j}\}$,

$$\forall t \in [t_{i-1,j}, t_{i,j}], \qquad \begin{aligned} v_{c_1}^{G_{1,i,j}}(t) &= v_{c_1}^{G_{1,i,j}}(\theta_{c_1,i,j}), \\ v_{c_2}^{G_{2,i,j}}(t) &= v_{c_2}^{G_{2,i,j}}(t_{i-1,j}). \end{aligned}$$

However, this assumption could result in some issues, e.g. intersecting trajectories, which is not realistic especially for a single-lane road. Moreover, with the assumption of constant speeds between D_j and D_{j+1}, there might be a great difference between the estimated time-mean speed of the vehicles at x_{j+1} and the reported value of the time-mean speed at x_{j+1} by loop detector D_{j+1} in the upcoming cycle.

Therefore, in this section we will relax the assumption of having a constant speed for each vehicle that travels between two consecutive loop detectors using Newell's car-following model (Newell 2002). In this model, the mathematical relationship between trajectories of vehicle c (leader) and vehicle $c+1$ (follower) are given. Applying Newell's model, we can find trajectories with partly piecewise linear behaviors. It is assumed that vehicle $c+1$ adapts its speed to the speed of the leading vehicle c in the time–space plane after a delay (see Figure 8).
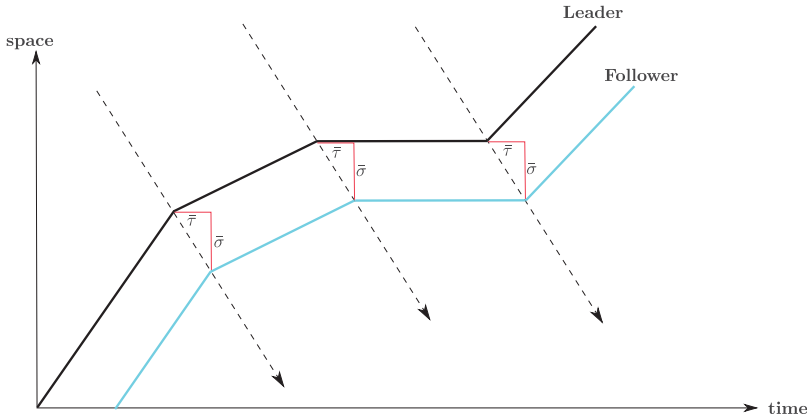

Figure 8. Trajectory of a following vehicle with respect to the leading vehicle applying Newell's car-following model.

Newell proposes that trajectories of the leading and the following vehicles are separated by a temporal distance of τ_c and a spatial distance of σ_c in the time–space plane; mathematically speaking, for a leading and a following vehicle within window $w_{i,j}$

$$x_{c-1,i,j}(t) = x_{c,i,j}(t + \tau_c) + \delta_c, \quad t \in [t_{i-1,j}, t_{i,j}]. \tag{49}$$

The parameters σ_c and τ_c might vary from driver to driver, considering different driving behaviors.[2] Each driver chooses the spatial distance σ_c based on their feeling of the safe distance from the front vehicle on the road; τ_c shows the delay time of a driver in responding to any external stimuli. For the sake of simplicity, we consider the average values of σ_c and τ_c shown by $\bar{\sigma}$ and $\bar{\tau}$ for all vehicles, i.e.

$$\forall c_1 \in \{1, \ldots, N_{1,i,j}\} \quad \text{and} \quad \forall c_2 \in \{1, \ldots, N_{2,i,j}\}, \qquad \begin{aligned} \bar{\tau} &= \sum_{g=1}^{2} \left(\frac{1}{N_{g,i,j}} \sum_{c=1}^{N_{g,i,j}} \tau_c \right), \\ \bar{\sigma} &= \sum_{g=1}^{2} \left(\frac{1}{N_{g,i,j}} \sum_{c=1}^{N_{g,i,j}} \sigma_c \right). \end{aligned} \tag{50}$$

Alternatively, we propose an estimation method for trajectories of the vehicles, applying Newell's car-following model to the sampling windows $w_{i,j}$, for $i \in \{1, \ldots, n_j^{\text{cyc}}\}$ and $j \in \{1, \ldots, n^{\text{loop}}\}$ in the time–space plane. First, we should find the leading vehicle in window $w_{i,j}$; the vehicle in $G_{2,i,j}$ that has the largest $s_{c_2}^{\text{start},G_{2,i,j}}$ is the leader; note that if $G_{2,i,j} = \emptyset$, then the vehicle in $G_{1,i,j}$ that arrives first in $w_{i,j}$, i.e. $c_1 = 1$, will be the leading vehicle in this window. We denote the leading vehicle by c^{leader}. Then we consider c^{follower} as the index for the following vehicle, which for $G_{2,i,j} \neq \emptyset$ should satisfy

$$s_{c^{\text{follower}}}^{\text{start},G_{2,i,j}} = \max_{c_2 \in \mathcal{N}_{2,i,j}/\{c^{\text{leader}}\}} \{s_{c_2}^{\text{start},G_{2,i,j}}\}, \quad \mathcal{N}_{2,i,j} = \{1, \ldots, N_{2,i,j}\},$$

or should be the second arriving vehicle in $w_{i,j}$ if $G_{2,i,j} = \emptyset$ (i.e. $c_1 = 2$).

First, we define

$$\begin{aligned} t_{\text{follower}}^{\text{ent},G_{1,i,j}} &= \theta_{c^{\text{follower}},i,j}, \\ t_{\text{follower}}^{\text{ent},G_{2,i,j}} &= t_{i-1,j}, \\ t_{\text{leader}}^{\text{ent},G_{1,i,j}} &= \theta_{c^{\text{leader}},i,j}, \\ t_{\text{leader}}^{\text{ent},G_{2,i,j}} &= t_{i-1,j}, \end{aligned} \tag{51}$$

and $v_{\text{leader}}^{\text{init}}$ as the initial speed of the leading vehicle that might be either $v_{c^{\text{leader}}}^{G_{1,i,j}}(t_{\text{leader}}^{\text{ent},G_{1,i,j}})$ or $v_{c^{\text{leader}}}^{G_{2,i,j}}(t_{\text{leader}}^{\text{ent},G_{2,i,j}})$, and $v_{\text{follower}}^{\text{init}}$ as the initial speed of the following vehicle that might be either $v_{c^{\text{follower}}}^{G_{1,i,j}}(t_{\text{follower}}^{\text{ent},G_{1,i,j}})$ or $v_{c^{\text{follower}}}^{G_{2,i,j}}(t_{\text{follower}}^{\text{ent},G_{2,i,j}})$. Now for a leading vehicle that belongs to either $G_{1,i,j}$ or to $G_{2,i,j}$ in $w_{i,j}$ we obtain

- if $v_{\text{leader}}^{\text{init}} = v_{i,j}^{\text{free}}$, where by $v_{i,j}^{\text{free}}$ we mean the free-flow speed of the vehicles[3] on the sampling road section j during $[t_{i-1,j}, t_{i,j}]$, then the leading vehicle keeps moving forward with $v_{i,j}^{\text{free}}$ till it leaves $w_{i,j}$;
- if $v_{\text{leader}}^{\text{init}} \neq v_{i,j}^{\text{free}}$, then the vehicle accelerates with $a_{c^{\text{leader}}}^{\text{max}}$, i.e. the maximum possible acceleration rate for this vehicle, to obtain $v_{i,j}^{\text{free}}$; then it keeps moving with $v_{i,j}^{\text{free}}$ till it leaves $w_{i,j}$.
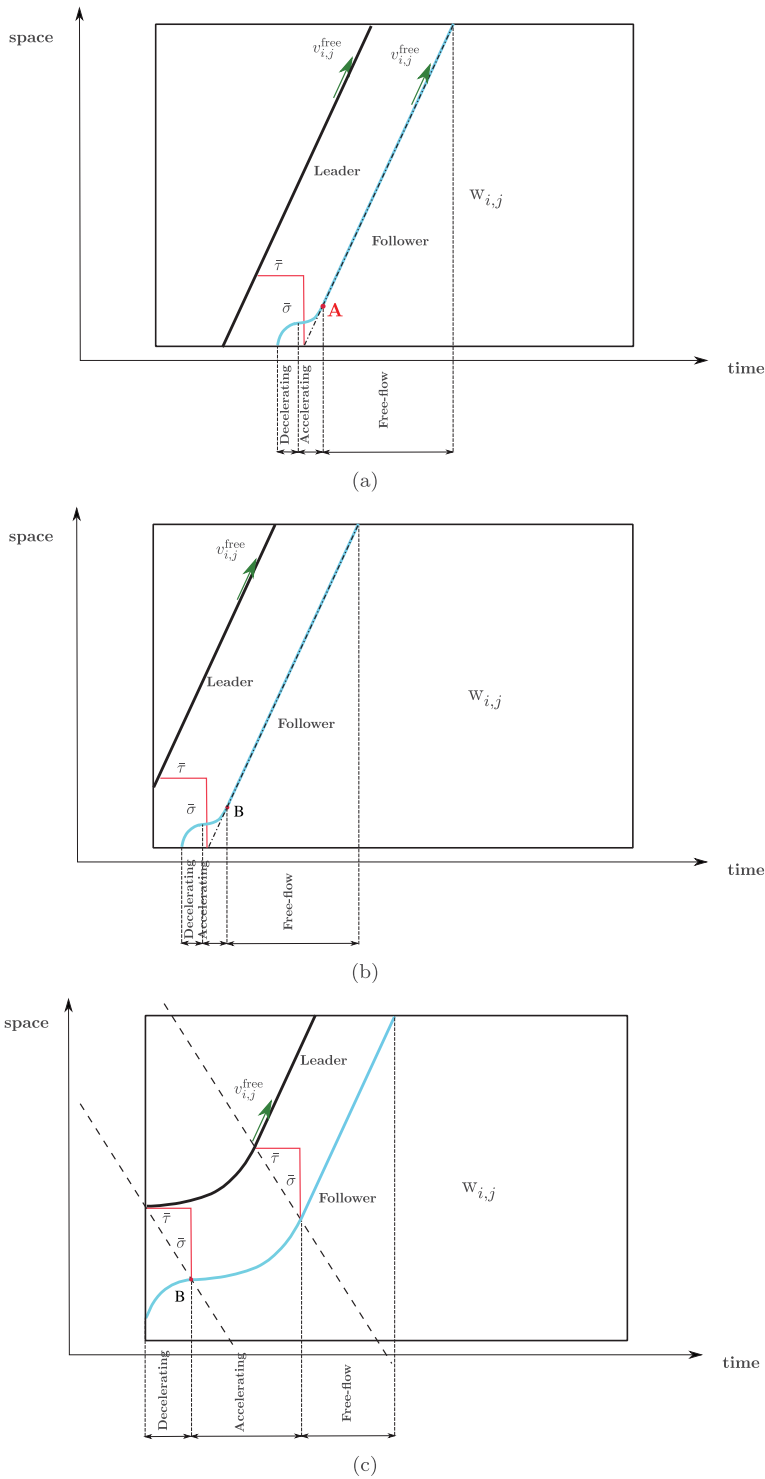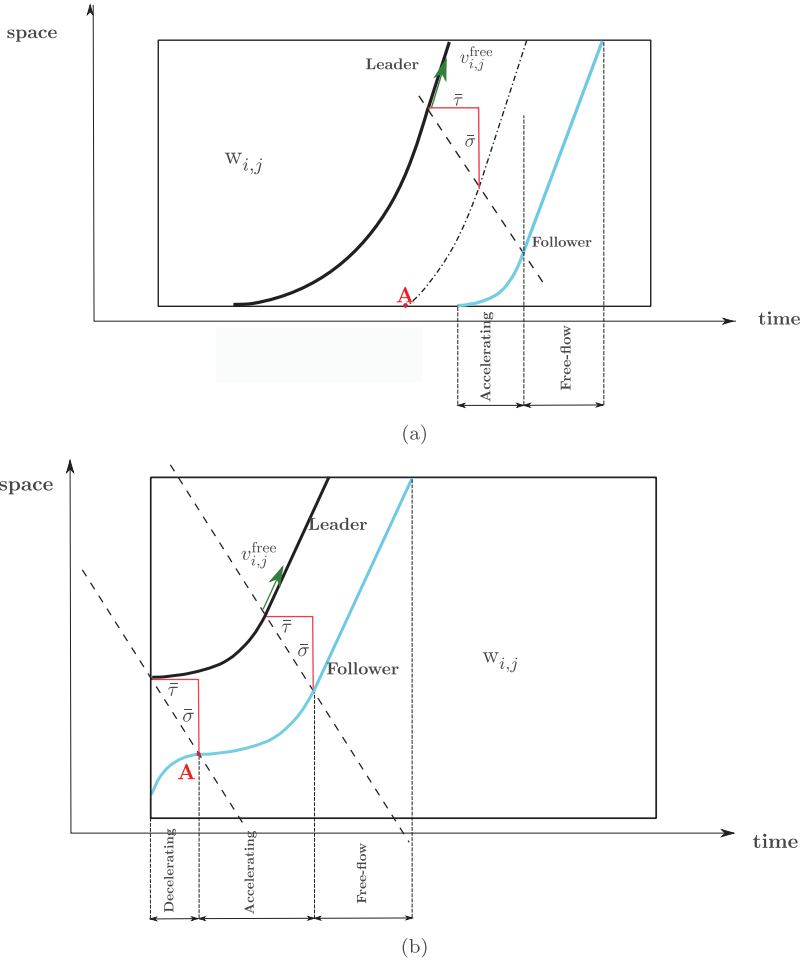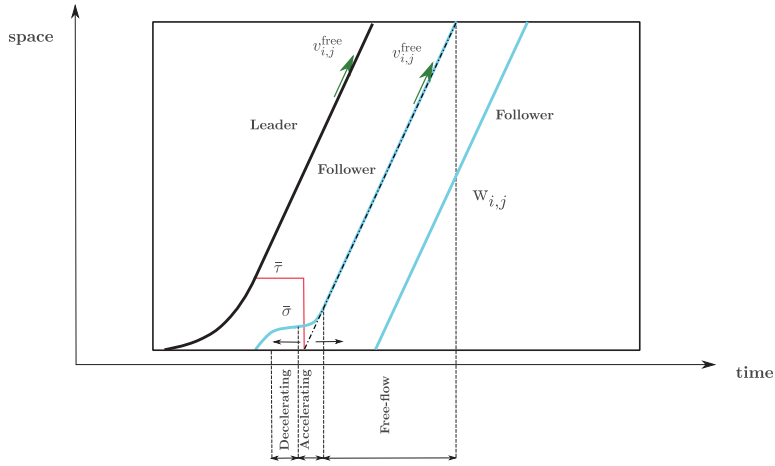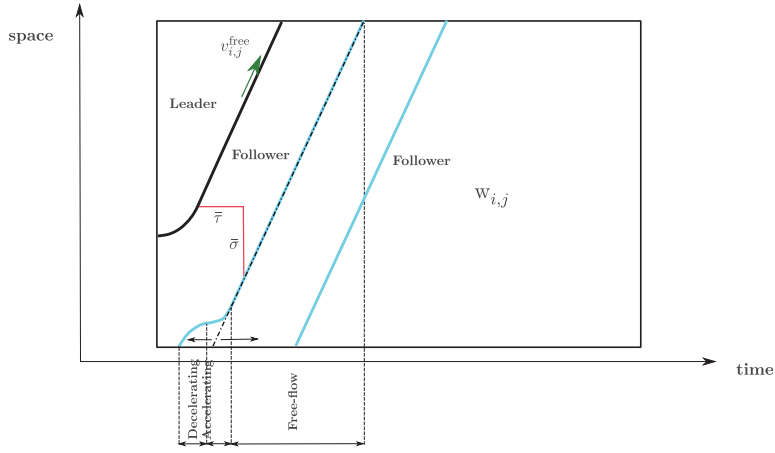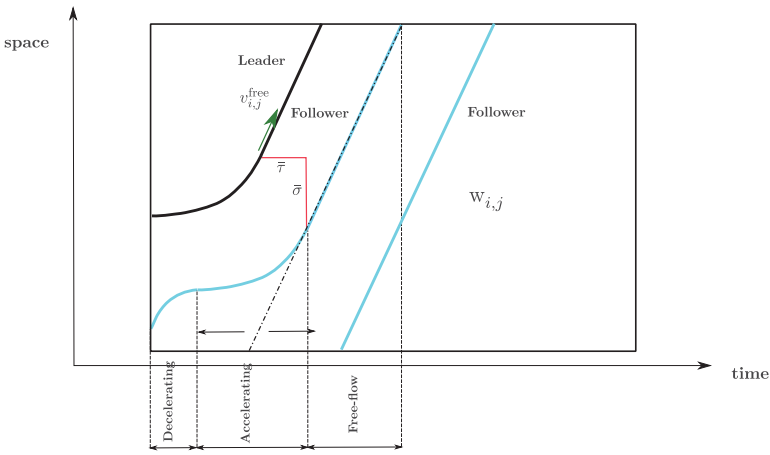
Figure 9. Behavior of the leading and following vehicles in $w_{i,j}$ for $v_{\text{leader}}^{\text{init}} = v_{i,j}^{\text{free}}$. (a) Trajectories of the leader and the follower both from $G_{1,i,j}$. (b) Trajectories of the leader from $G_{2,i,j}$ and the follower from $G_{1,i,j}$. (c) Trajectories of the leader and the follower with $v_{\text{follower}}^{\text{init}} < v_{i,j}^{\text{free}}$.

For the following vehicle, three situations might be observed, i.e.

Situation 1. The leading and the following vehicles both belong to $G_{1,i,j}$,
Situation 2. The leading and the following vehicles both belong to $G_{2,i,j}$,
Situation 3. The leading vehicle belongs to $G_{2,i,j}$, while the following vehicle belongs to $G_{1,i,j}$.

Consequently, we obtain

- if $v_{\text{follower}}^{\text{init}} = v_{i,j}^{\text{free}}$ and $v_{\text{leader}}^{\text{init}} = v_{i,j}^{\text{free}}$, for situation 1, situation 2, and situation 3 we assume that the following vehicle keeps moving forward with $v_{i,j}^{\text{free}}$ till it leaves the window. However, if for situation 1 we observe

$$\theta_{c^{\text{follower},i,j}} - \theta_{c^{\text{leader},i,j}} < \bar{\tau},$$

or if for situation 3 either of the following relationships hold:

$$\theta_{c^{\text{follower},i,j}} - t_{i-1,j} < \bar{\tau} \quad \text{or} \quad s_{c^{\text{leader}}}^{\text{start},G_2,G_{2,i,j}} < \bar{\sigma},$$

Figure 10. Behavior of the leading and following vehicles in $w_{i,j}$ for $v_{\text{leader}}^{\text{init}} < v_{i,j}^{\text{free}}$. (a) Trajectories of the leader and the follower both from $G_{1,i,j}$. (b) Trajectories of the leader and the follower both from $G_{2,i,j}$.

Figure 11. Behavior of the leading and following vehicles in $w_{i,j}$ for $v_{\text{leader}}^{\text{init}} < v_{\text{follower}}^{\text{init}}$. (a) Trajectories of the leader and the follower both from $G_{1,i,j}$. (b) Trajectories of the leader from $G_{2,i,j}$ and the follower from $G_{1,i,j}$. (c) Trajectories of the leader both from $G_{2,i,j}$.

then the following vehicle will first decelerate and then accelerates such that it adjusts the temporal and/or the spatial distances of its trajectory from the one of the leader, to the values $\bar{\tau}$ and $\bar{\sigma}$, respectively (see Figure 9(a) and 9(b)).

- If $v_{\text{follower}}^{\text{init}} < v_{i,j}^{\text{free}}$ and $v_{\text{leader}}^{\text{init}} = v_{i,j}^{\text{free}}$, then for situation 1, 2 and 3 the follower will accelerate with the maximum acceleration rate, and after reaching $v_{i,j}^{\text{free}}$ it keeps moving forward with $v_{i,j}^{\text{free}}$ till it leaves $w_{i,j}$ (see Figure 9(c)). If the initial temporal and spatial distances of the trajectory of the following vehicle in $w_{i,j}$ from the initial point of the trajectory of the leading vehicle in $w_{i,j}$ are less than $\bar{\tau}$ and $\bar{\sigma}$, we assume that the following vehicle adjusts its acceleration such that it reaches $v_{i,j}^{\text{free}}$ at a point where its trajectory is located at a temporal and spatial distance of $\bar{\tau}$ and $\bar{\sigma}$ from the trajectory of the leading vehicle.

- If $v_{\text{follower}}^{\text{init}} < v_{i,j}^{\text{free}}$ and $v_{\text{leader}}^{\text{init}} < v_{i,j}^{\text{free}}$, then the following vehicle will accelerate with the maximum acceleration rate, and after reaching $v_{i,j}^{\text{free}}$ it keeps moving forward with $v_{i,j}^{\text{free}}$ till it leaves $w_{i,j}$. The following vehicle should make sure that it reaches $v_{i,j}^{\text{free}}$ at a point which is located in a temporal and spatial distance of $\bar{\tau}$ and $\bar{\sigma}$ or more, from the point on the trajectory of the leading vehicle, at which the leading vehicle reaches $v_{i,j}^{\text{free}}$ (see Figure 10(a) and 10(b)).

- If $v_{\text{follower}}^{\text{init}} = v_{i,j}^{\text{free}}$ and $v_{\text{leader}}^{\text{init}} < v_{i,j}^{\text{free}}$, then depending on the initial relative temporal and spatial distances of the trajectories of the leading and following vehicles, different behaviors might be observed for the following vehicle; Figure 11(a)–(c) illustrate three possible situations, in which $c^{\text{leader}} \in G_{1,i,j}$ and $c^{\text{follower}} \in G_{1,i,j}$, $c^{\text{leader}} \in G_{2,i,j}$ and $c^{\text{follower}} \in G_{1,i,j}$, and $c^{\text{leader}} \in G_{2,i,j}$ and $c^{\text{follower}} \in G_{2,i,j}$. For either of these three possibilities, if the following vehicle is located on the left-hand side of the dash-dotted curve shown in Figure 11(a)–(c), then the vehicle first decelerates and then accelerates such that its speed reaches $v_{i,j}^{\text{free}}$ again at the instant its trajectory intersects the dash-dotted curve. Otherwise, the following vehicle can freely keep moving forward with $v_{i,j}^{\text{free}}$ from the beginning of the cycle. Mathematically speaking, these three conditions can be formulated as follows:

(1) If $c^{\text{leader}} \in G_{1,i,j}$ and $c^{\text{follower}} \in G_{1,i,j}$ (see Figure 11(a)),

$$\theta_{c^{\text{follower}},i,j} \geq \theta_{c^{\text{leader}},i,j} + \theta^{\text{acc}} + \bar{\tau} \Rightarrow \text{the following vehicle keeps moving with } v_{i,j}^{\text{free}};$$

otherwise, the following vehicle will first decelerate.

(2) If $c^{\text{leader}} \in G_{2,i,j}$ and $c^{\text{follower}} \in G_{1,i,j}$ (see Figure 11(b)),

$$\theta_{c^{\text{follower}},i,j} \geq t_{i-1,j} + \theta^{\text{acc}} + \bar{\tau} \Rightarrow \text{the following vehicle keeps moving with } v_{i,j}^{\text{free}};$$

otherwise, the following vehicle will first decelerate.

(3) If $c^{\text{leader}} \in G_{2,i,j}$ and $c^{\text{follower}} \in G_{2,i,j}$ (see Figure 11(c)),

$$s_{c^{\text{follower}}}^{\text{start},G_{2,i,j}} \geq v_{i,j}^{\text{free}}(t_{i-1,j} - \theta^{\text{acc}} - \bar{\tau}) + s_{c^{\text{leader}}}^{\text{start},G_{2,i,j}} + d^{\text{acc}} - \bar{\delta} \Rightarrow$$

the following vehicle keeps moving with $v_{i,j}^{\text{free}}$; otherwise, the following vehicle will first decelerate.

6. Results

In this section, we present the results of a case study that uses the real-life datasets of NGSIM. These datasets are available on either of the following three websites:

(1) http://www.ngsim-community.org/,
(2) http://gateway.path.berkeley.edu/ngsimdocs/US-101/,
(3) http://gateway.path.berkeley.edu/ngsimdocs/I-80/,

and provide detailed information including the positions and the speeds of individual vehicles. For our experiment in this paper, we have used the datasets that are available on the third website. These datasets have been generated as part of the NGSIM project by the Federal Highway Administration, from a segment of the interstate freeway I-80 in San Francisco, California, USA, on 13 April 2005. The data have been collected via seven video cameras from 2.00 PM till 7.00 PM, and is available in three sets for the time periods between 4.00 PM and 4.15 PM, between 5.00 PM and 5.15 PM, and between 5.15 PM and 5.30 PM. We indicate these three datasets by 'dataset 1', 'dataset 2', and 'dataset 3', respectively.

From these datasets, we can extract the trajectories of the vehicles and compute the real value of the generalized average speed. To assess the efficiency of the proposed sequential algorithm, we use
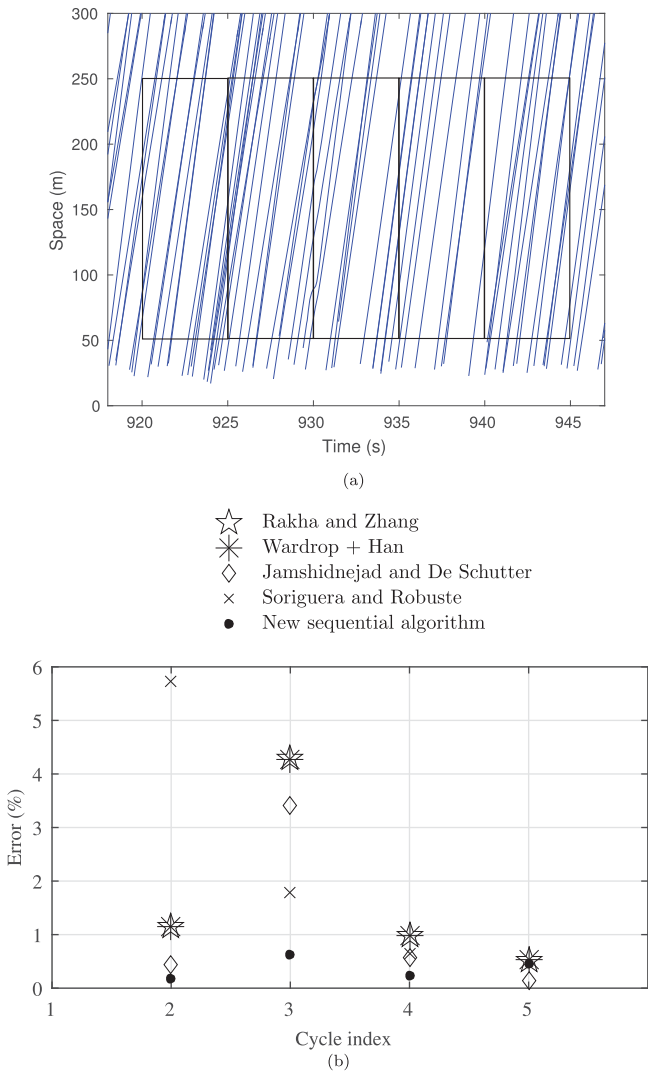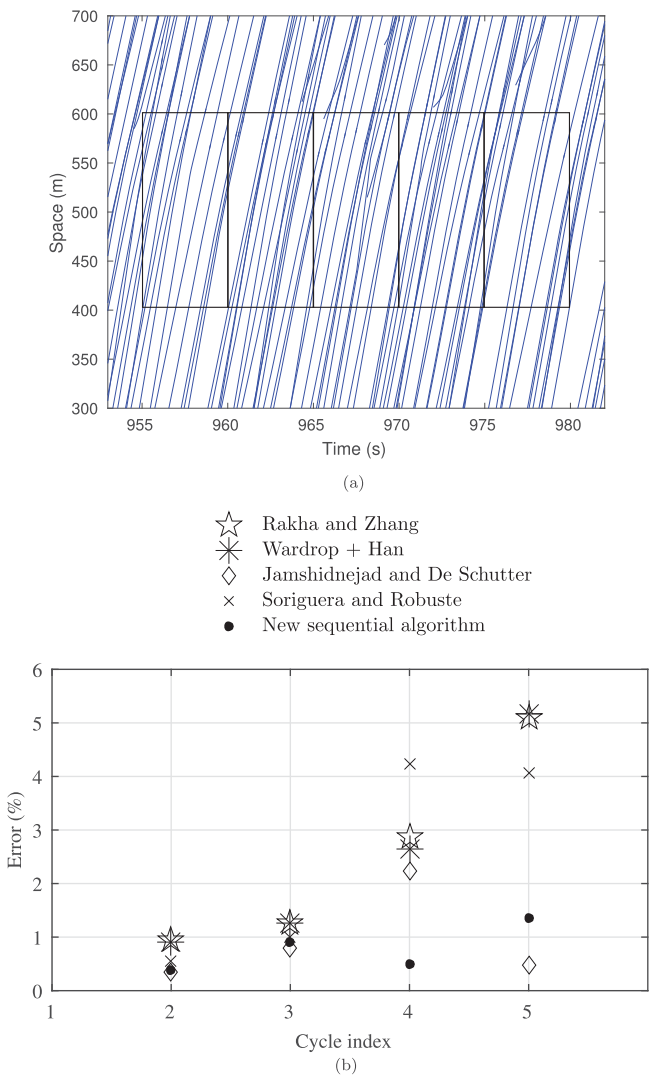

Figure 12. *Dataset 1, first sampling road section:* trajectories and relative errors w.r.t. the real value of the generalized average speed for the formulas given by Rakha and Zhang (2005), by Wardrop (1952) and Han et al. (2010), by Jamshidnejad and De Schutter (2015), by Soriguera and Robusté (2011), and by the new sequential algorithm. (a) Trajectories of the vehicles and the sampling windows. (b) Relative errors in percentage.

it to determine the generalized average speed of the vehicles. Moreover, we implement the formulas given by Wardrop (1952) and by Han et al. (2010), by Rakha and Zhang (2005), by Soriguera and Robusté (2011), and by Jamshidnejad and De Schutter (2015) as a comparison, since these papers represent the state-of-the-art for estimation of the classical and the generalized average speed of the vehicles. The formulas proposed by Wardrop (1952) and by Rakha and Zhang (2005) are the most well-known formulas in the literature for estimating the space-mean speed of the vehicles a road. Han et al. (2010) and Soriguera and Robusté (2011) give formulas for estimating the, respectively, spatial and temporal standard deviation of the speeds of the observed vehicles. The spatial standard deviation can be used in the formula by Wardrop (1952) to estimate the space-mean speed of the vehicles, while the temporal standard deviation in combination with the formula by Rakha and Zhang (2005) gives the estimated space-mean speed of the vehicles. Since all these formulas estimate the space-mean
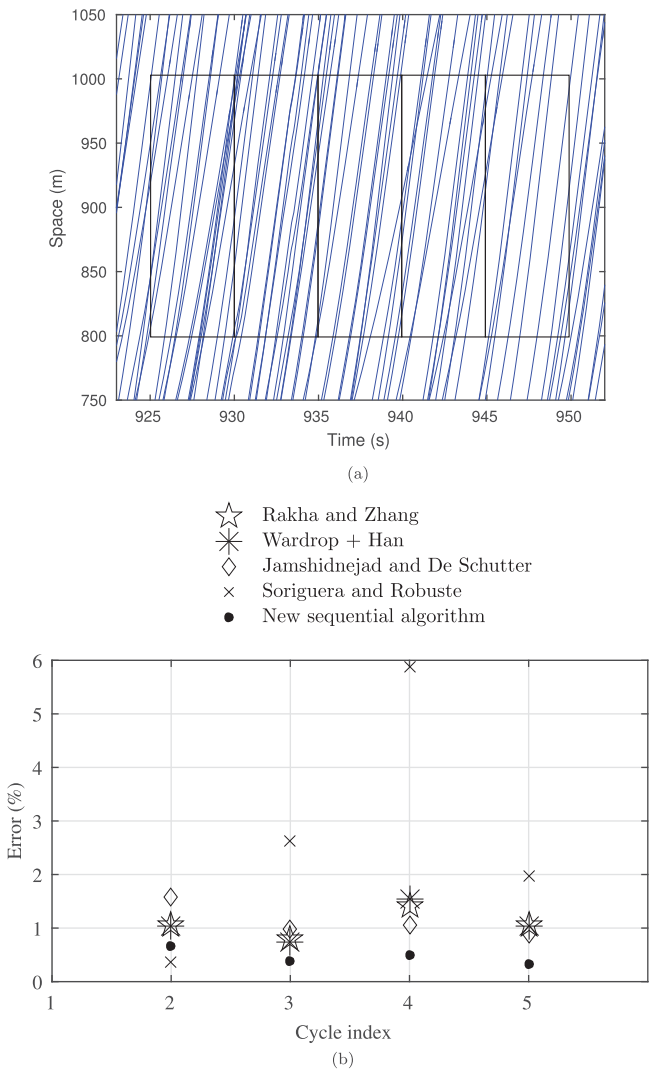

Figure 13. *Dataset 1, second sampling road section:* trajectories and relative errors w.r.t. the real value of the generalized average speed for the formulas given by Rakha and Zhang (2005), by Wardrop (1952) and Han et al. (2010), by Jamshidnejad and De Schutter (2015), by Soriguera and Robusté (2011), and by the new sequential algorithm. (a) Trajectories of the vehicles and the sampling windows. (b) Relative errors in percentage.

speed, we can observe how in some cases the estimated value of the space-mean speed is close to the real value of the generalized average speed, while in other cases the estimated space-mean speed can deviate significantly from the real generalized average speed. Additionally, we use the formula given by Jamshidnejad and De Schutter (2015) as the only available formula that takes into account estimation of the generalized average speed from point measurements. This formula has proven to be very accurate compared with other formulas (see Jamshidnejad and De Schutter 2015), and hence, it can provide a good comparison case for the proposed approach in this paper.

For this case study, we extracted those sections of the trajectory plots from the NGSIM datasets, for which enough information was available, as the dataset gives the trajectories for some time intervals, and then there are gaps between these intervals where no trajectories are available. For each of the three datasets, we could extract four cases, i.e. four different sampling road sections. Since the length
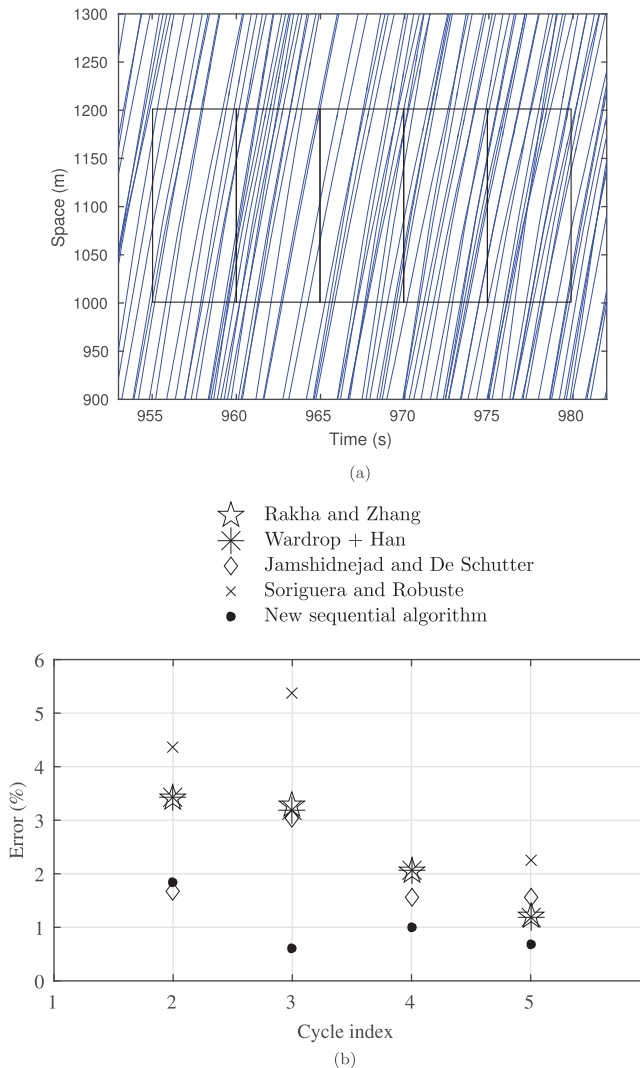

Figure 14. *Dataset 1, third sampling road section:* trajectories and relative errors w.r.t. the real value of the generalized average speed for the formulas given by Rakha and Zhang (2005), by Wardrop (1952) and Han et al. (2010), by Jamshidnejad and De Schutter (2015), by Soriguera and Robusté (2011), and by the new sequential algorithm. (a) Trajectories of the vehicles and the sampling windows. (b) Relative errors in percentage.

of the time intervals, for which trajectories were available are short, we decided to choose sampling windows of dimensions $L_j = 150$ m and 200 m by $T_j = 5$ s. This way we could obtain five successive sampling windows for each of the four selected cases that are illustrated in Figures 12(a)–15(a) for dataset 1, Figures 16(a)–19(a) for dataset 2, and Figures 20(a)–23(a) for dataset 3.

As it was indicated before, we have considered four different sampling road sections for each dataset. For dataset 1, the starting and end points of the first sampling road section are located at $x_{1,1}^u = 50$ m and $x_{1,1}^d = 250$ m (see Figure 12(a)), with the upstream and downstream loop detectors located at $x_{1,1}^u$ and $x_{1,1}^d$, respectively. The second sampling road section (see Figure 13(a)) corresponds to the starting and end points $x_{1,2}^u = 400$ m and $x_{1,2}^d = 600$ m, with the upstream and downstream loop detectors at $x_{1,2}^u$ and $x_{1,2}^d$. The third sampling road section (see Figure 14(a)) starts at $x_{1,3}^u = 800$ m and ends at $x_{1,3}^d = 1000$ m, where the upstream loop detector is located at $x_{1,3}^u$ and the downstream
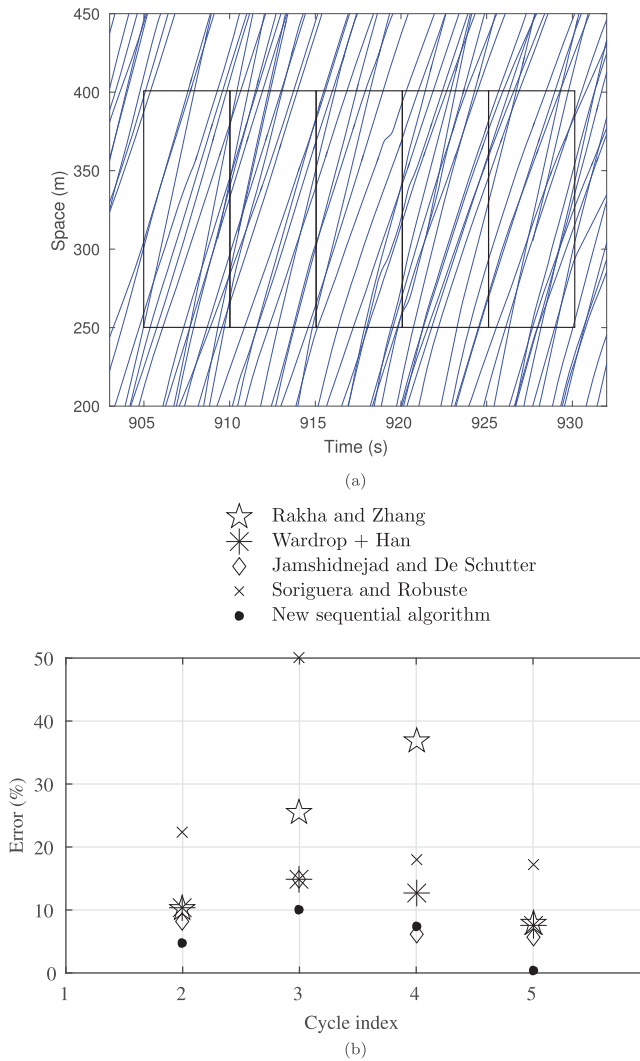

Figure 15. *Dataset 1, fourth sampling road section:* trajectories and relative errors w.r.t. the real value of the generalized average speed for the formulas given by Rakha and Zhang (2005), by Wardrop (1952) and Han et al. (2010), by Jamshidnejad and De Schutter (2015), by Soriguera and Robusté (2011), and by the new sequential algorithm. (a) Trajectories of the vehicles and the sampling windows. (b) Relative errors in percentage.

loop detector is located at $x^d_{1,3}$. Finally, the fourth sampling road section (see Figure 15(a)) has the starting and end points at $x^u_{1,4} = 1000$ m and $x^d_{1,4} = 1200$ m, with the upstream and downstream loop detectors located at $x^u_{1,4}$ and $x^d_{1,4}$. The time interval considered for the first sampling road section is between $t = 920$ s and $t = 945$ s (see Figure 12(a)), for the second sampling road section it is between $t = 955$ s and $t = 980$ s (see Figure 13(a)), for the third sampling road section it is between $t = 925$ s and $t = 950$ s (see Figure 14(a)), and for the fourth sampling road section it is between $t = 955$ s and $t = 980$ s (see Figure 15(a)).

For dataset 3, the first sampling road section (see Figure 20(a)) corresponds to $x^u_{3,1} = 950$ m and $x^d_{3,1} = 1150$ m, and the time interval between $t = 1875$ s and $t = 1900$ s . The second sampling road section (see Figure 21(a)) corresponds to $x^u_{3,2} = 1300$ m and $x^d_{3,2} = 1450$ m, and the time interval
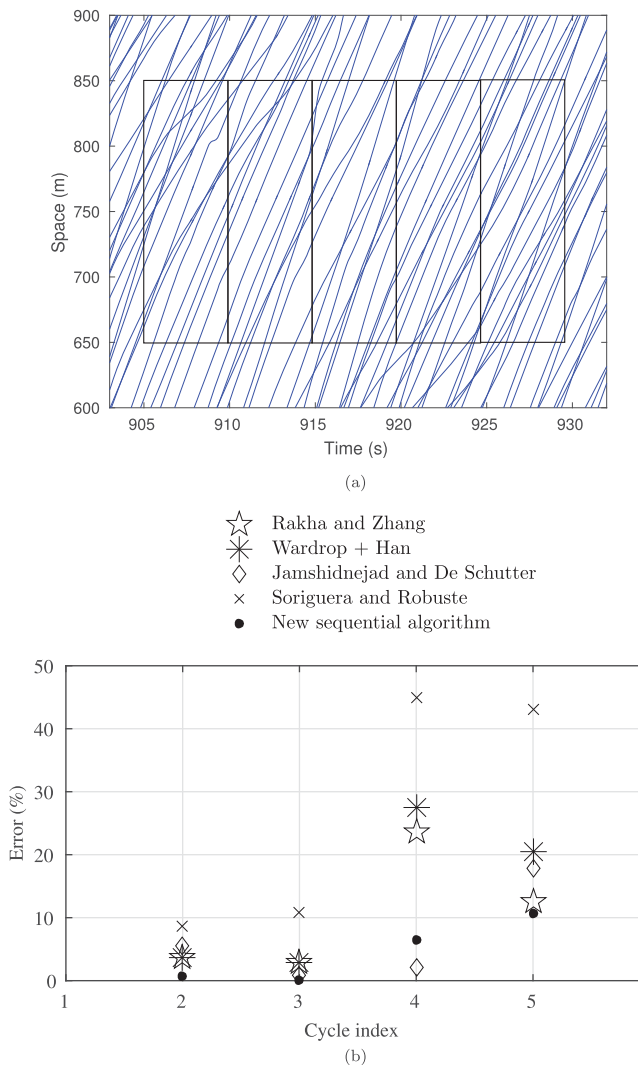

Figure 16. *Dataset 2, first sampling road section:* trajectories and relative errors w.r.t. the real value of the generalized average speed for the formulas given by Rakha and Zhang (2005), by Wardrop (1952) and Han et al. (2010), by Jamshidnejad and De Schutter (2015), by Soriguera and Robusté (2011), and by the new sequential algorithm (note that for the third window, the error of the formula by Soriguera and Robusté 2011 exceeds 50%, but for the illustration purposes we have shown it at 50%). (a) Trajectories of the vehicles and the sampling windows. (b) Relative errors in percentage.

between $t = 2400$ s and $t = 2425$ s. The third sampling road section (see Figure 22(a)) corresponds to $x_{3,3}^u = 150$ m and $x_{3,3}^d = 300$ m, and the time interval between $t = 1905$ s and $t = 1930$ s. The fourth sampling road section (see Figure 23(a)) corresponds to $x_{3,4}^u = 1000$ m and $x_{3,4}^d = 1150$ m, and the time interval $t = 2060$ s and $t = 2085$ s.

Figures 12(b)–15(b), 16(b)–19(b), and 20(b)–23(b) illustrate the relative errors w.r.t. the real value of the generalized average speed, which is computed by Equation (2), i.e. the ratio of the absolute difference between the generalized average speed and the computed average speed via each of the formulas (by Rakha and Zhang (2005), by Wardrop (1952) and Han et al. (2010), by Jamshidnejad and De Schutter (2015), by Soriguera and Robusté (2011), and by the new sequential algorithm), and the generalized average speed for datasets 1, 2, and 3, respectively. For the 12 cases shown in Figures 12–23, the errors corresponding to the first windows are not shown; because the main aim of the assessment
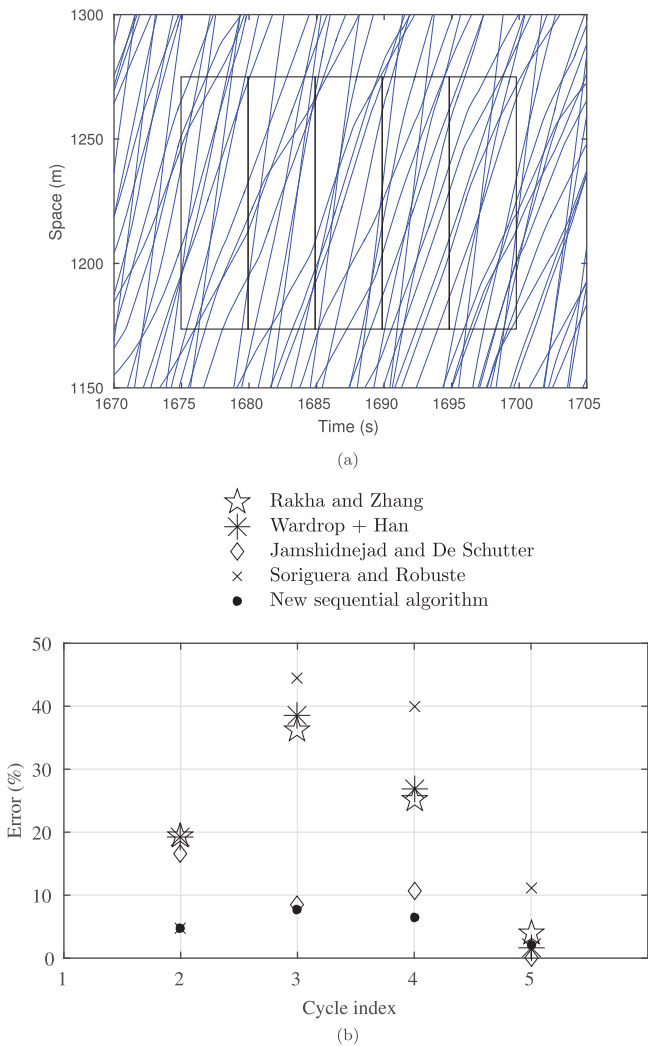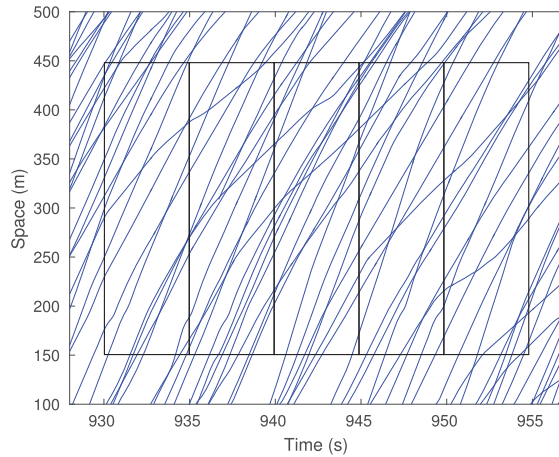

Figure 17. *Dataset 2, second sampling road section:* trajectories and relative errors w.r.t. the real value of the generalized average speed for the formulas given by Rakha and Zhang (2005), by Wardrop (1952) and Han et al. (2010), by Jamshidnejad and De Schutter (2015), by Soriguera and Robusté (2011), and by the new sequential algorithm. (a) Trajectories of the vehicles and the sampling windows. (b) Relative errors in percentage.

is to investigate the efficiency of the new sequential algorithm, including its capability for computing the initial conditions for the next sampling window and in using the computed initial conditions for the current sampling window. However, for the first windows in Figures 12(a)–23(a), the initial conditions are just given to the algorithm as an input of the problem, and therefore are not estimated by the algorithm itself. Hence, the first sampling windows in the four cases should not be considered for assessment of the algorithm.

From Figure 12(b), we see that the proposed sequential algorithm shows the best performance for the second, third, and fourth windows, while for the fifth window, the formula proposed by Jamshidnejad and De Schutter (2015) performs better. This can be explained by taking into account the main focus of each of these two approaches. Jamshidnejad and De Schutter (2015) mainly focus on each sampling window from a microscopic point-of-view, and make accurate computations for each sampling window via partitioning it into smaller windows. The new sequential algorithm proposed in this
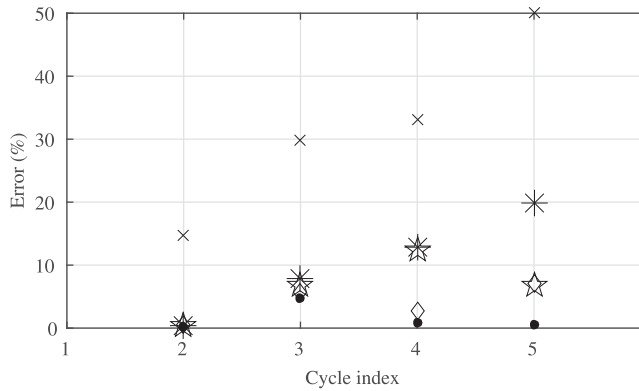

Figure 18. *Dataset 2, third sampling road section:* trajectories and relative errors w.r.t. the real value of the generalized average speed for the formulas given by Rakha and Zhang (2005), by Wardrop (1952) and Han et al. (2010), by Jamshidnejad and De Schutter (2015), by Soriguera and Robusté (2011), and by the new sequential algorithm. (a) Trajectories of the vehicles and the sampling windows. (b) Relative errors in percentage.
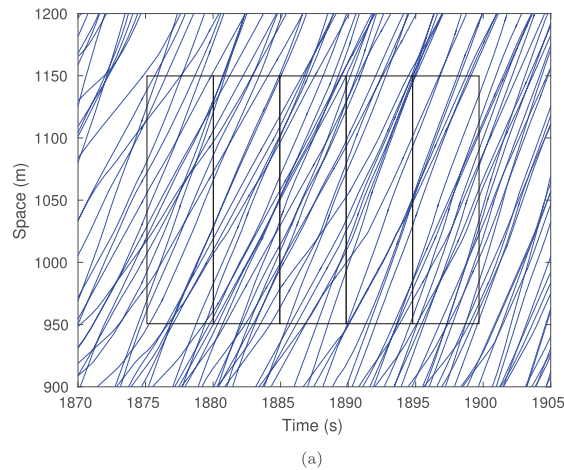
Figure 19. *Dataset 2, fourth sampling road section:* trajectories and relative errors w.r.t. the real value of the generalized average speed for the formulas given by Rakha and Zhang (2005), by Wardrop (1952) and Han et al. (2010), by Jamshidnejad and De Schutter (2015), by Soriguera and Robusté (2011), and by the new sequential algorithm (note that for the 5th window, the error of the formula by Soriguera and Robusté 2011 exceeds 50%, but for the illustration purposes we have shown it at 50%). (a) Trajectories of the vehicles and the sampling windows. (b) Relative errors in percentage.

paper, however, focuses on the common edges of the sampling windows within the time–space plane, and those trajectories that intersect these edges. Therefore, it does not go into a lot of details for each sampling window, but instead it considers the details regarding transition of vehicle trajectories from one sampling window to the neighboring window. Consequently, if there are more trajectories that intersect the common edge of two neighboring sampling windows, we expect the proposed algorithm to produce more accurate results compared with other approaches. In Figure 12(b), by considering the number of trajectories that intersect the left edges of the sampling windows w.r.t. the total number of trajectories observed in each of these windows, we see that for the second, third, and fourth windows, this ratio is much larger (between 27% and 50 %) than for the fifth window (6%). Therefore, we expect the effect of ignoring these trajectories in the computations to be more significant for the second, third, and fourth windows, and that the sequential algorithm shows a better performance. This
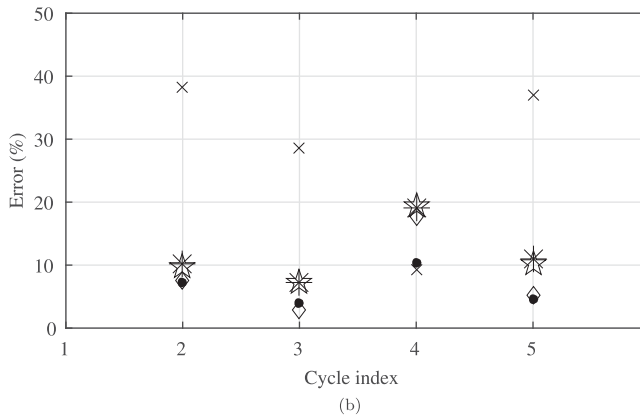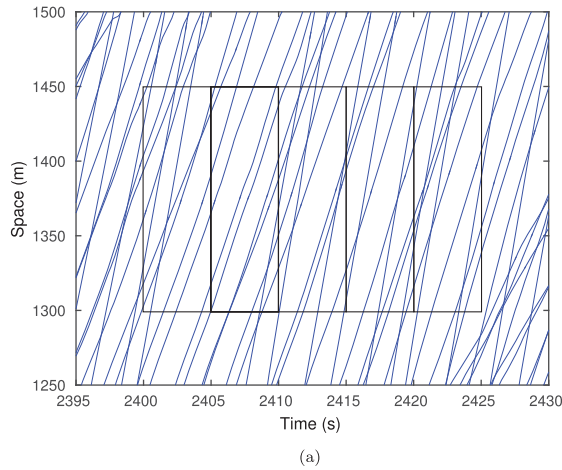

Figure 20. *Dataset 3, first sampling road section:* trajectories and relative errors w.r.t. the real value of the generalized average speed for the formulas given by Rakha and Zhang (2005), by Wardrop (1952) and Han et al. (2010), by Jamshidnejad and De Schutter (2015), by Soriguera and Robusté (2011), and by the new sequential algorithm. (a) Trajectories of the vehicles and the sampling windows. (b) Relative errors in percentage.

expectation is well supported by the results illustrated in Figure 12(b). Moreover, from Figure 12, we see that when the formula proposed by Soriguera and Robusté (2011) is combined with the formula by Rakha and Zhang (2005), it produces more accurate results for three out of four experiments (see the results corresponding to the third, fourth, and fifth windows).

In Figure 13(b), the performance of the new sequential algorithm and the formula by Jamshidnejad and De Schutter (2015) are very close, i.e. for some windows the new sequential algorithm shows the best performance, and for some other windows the formula by Jamshidnejad and De Schutter (2015) works better. For this case we see that, on the one hand, there is a relatively large number of vehicles, for which the trajectory intersects the right-hand edge of the sampling windows. On the other hand, there are some vehicles that change their speed while traveling within the sampling windows (i.e. their trajectories do not have a straight linear shape). Since the sequential algorithm covers the first issue (intersecting trajectories) and the formula by Jamshidnejad and De Schutter (2015) uses a convex
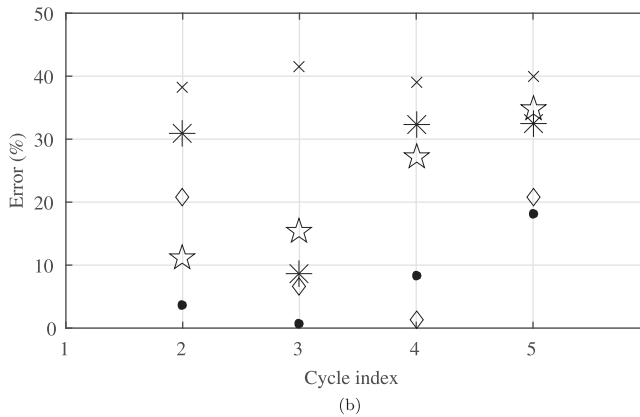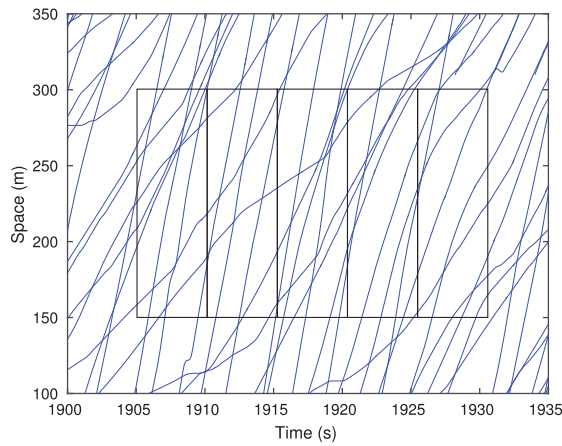
Figure 21. *Dataset 3, second sampling road section:* trajectories and relative errors w.r.t. the real value of the generalized average speed for the formulas given by Rakha and Zhang (2005), by Wardrop (1952) and Han et al. (2010), by Jamshidnejad and De Schutter (2015), by Soriguera and Robusté (2011), and by the new sequential algorithm. (a) Trajectories of the vehicles and the sampling windows. (b) Relative errors in percentage.

combination of the lower and upper bounds of the generalized average speed (see Section 2.2), we can expect to see such a close performance for these two approaches.

In Figure 14(b), for three out of the four sampling windows the best results correspond to the new sequential algorithm. As we see from the curves of trajectories, the ratio of the trajectories intersecting the left edge of each window and the total number of trajectories in that window is relatively large (between 23% and 40%). Therefore, we could expect the new sequential algorithm, which keeps track of the trajectories that intersect the left edge of the sampling windows, to produce the best results. For Figure 15(b), in three out of four windows, the sequential algorithm shows a significantly better performance, while for one window the formula by Jamshidnejad and De Schutter (2015) more accurate (note that the performance of the sequential algorithm proposed in this paper is still very close to the performance of the formula by Jamshidnejad and De Schutter 2015).
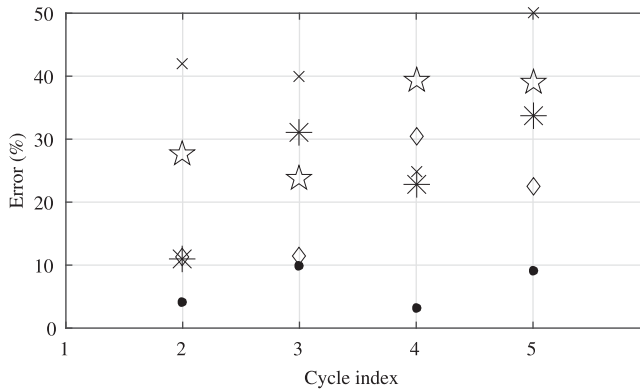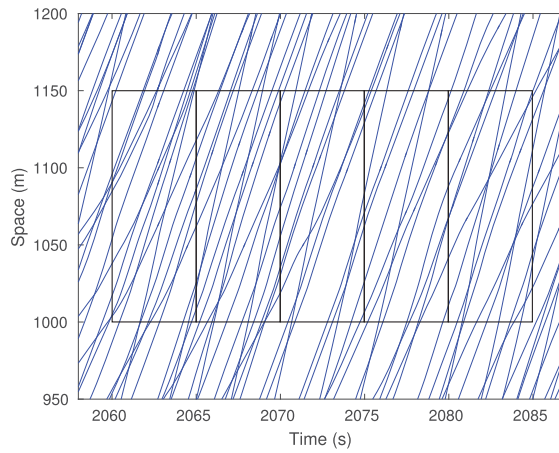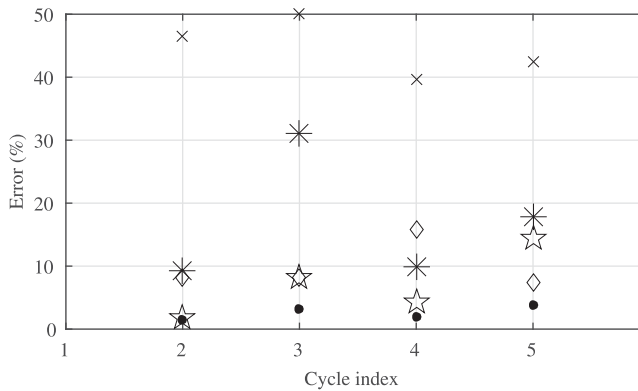
Figure 22. *Dataset 3, third sampling road section:* trajectories and relative errors w.r.t. the real value of the generalized average speed for the formulas given by Rakha and Zhang (2005), by Wardrop (1952) and Han et al. (2010), by Jamshidnejad and De Schutter (2015), by Soriguera and Robusté (2011), and by the new sequential algorithm. (a) Trajectories of the vehicles and the sampling windows. (b) Relative errors in percentage.

Figures 16–19, which correspond to dataset 2, show that in 12 cases out of 16 cases (i.e. in 75% of the cases), the proposed sequential algorithm exhibits the best performance, and for 3 out of 16 cases the formula by Jamshidnejad and De Schutter (2015) performs better. From Figures 20 to 23, which correspond to dataset 3, in 13 cases out of 16 cases (i.e. in 81.25% of the cases), the proposed sequential algorithm performs the best. Note that compared with the results obtained for dataset 1, where the relative error of the different formulas is always less than 6%, for datasets 2 and 3 this error may become close to or even exceed 50% for some formulas (but it never happens for the proposed sequential algorithm). In particular, in a few cases, for example for dataset 2, the third window of case 1 (see Figure 16(b)) and the fifth window of case 4 (see Figure 19(b)), and for dataset 3, the fifth window of case 3 (see Figure 22(b)) and the third window of case 4 (see Figure 23(b)), for the formula proposed by Soriguera and Robusté (2011) combined with the formula by Rakha and Zhang (2005) this error exceeds 50%. However, for the illustration purposes we have shown it at the highest percentage

Figure 23. *Dataset 3, fourth sampling road section:* trajectories and relative errors w.r.t. the real value of the generalized average speed for the formulas given by Rakha and Zhang (2005), by Wardrop (1952) and Han et al. (2010), by Jamshidnejad and De Schutter (2015), by Soriguera and Robusté (2011), and by the new sequential algorithm. (a) Trajectories of the vehicles and the sampling windows. (b) Relative errors in percentage.

used for the illustrations (i.e. 50%). In all these cases, however, the relative error of the proposed sequential algorithm almost never exceeds 10% (except for the fifth window of case 2 of dataset 3 (see Figure 21(b))), where the relative error of the proposed sequential algorithm reaches almost 18%; note, however, that this is still the lowest percentage among all the formulas.

In general, considering Figures 12–23, we see that the new sequential algorithm shows excellent performance in most cases compared to the other formulas. In most experiments, either the new sequential procedure or the formula by Jamshidnejad and De Schutter (2015) produce the most accurate results, while the other formulas are less accurate. For situations in which the formula by Jamshidnejad and De Schutter (2015) is more accurate, the difference between its result and the result of the sequential algorithm is rather small (less than 5%). However, for the cases where the sequential algorithm is the most accurate approach, the difference between the results produced by the algorithm and by the formula by Jamshidnejad and De Schutter (2015) is larger, i.e.

the error difference could be more than 10% based on the results of the case study (e.g. see the fifth window of Figure 22(b)). The combination of the formulas given by Rakha and Zhang (2005) and by Soriguera and Robusté (2011) shows the best performance in 2 out of the 48 experiments (the proposed sequential algorithm in these cases ranks second, with the difference of the errors of the combined formula by Rakha and Zhang 2005 and by Soriguera and Robusté 2011 , and the sequential algorithm less than 0.3%), and in 1 case out of 48 cases, both the proposed sequential algorithm and the combined formula by Rakha and Zhang (2005) and Soriguera and Robusté (2011) perform best.

7. Conclusions and future work

In this paper, a new sequential algorithm has been proposed for finding an accurate estimate of the generalized traffic fundamental variables (i.e. the generalized density, flow, and average speed), taking into account the effect of those vehicles that remain on the same sampling road section for more than one sampling cycle. The algorithm has been developed for both single-lane and multi-lane roads. In addition, we have also presented an approach that produces approximate trajectories of the vehicles in each sampling window using Newell's car-following model.

The results of the case study, which has used the real-life dataset NGSIM, show the excellent performance of the new sequential algorithm compared with other available formulas in the literature. In some situations, the microscopic formula by Jamshidnejad and De Schutter (2015) performs better than the new sequential algorithm. Consequently, we propose as a topic for future work to consider the possibility of combining the microscopic formula given by Jamshidnejad and De Schutter (2015) with the new sequential algorithm proposed in this paper. As a second topic for future work, we suggest to combine the approach for finding approximate trajectories of vehicles based on Newell's car-following model proposed in this paper with a lane-changing model to also take into account effects of lane change. Finally, we can consider situations where measurements of the loop detectors are noisy and see how efficient the proposed method is or what are the modifications we might need to make to improve the method for noisy measurements.

Notes

1. Note that for $i = 1$, the $s_{c_2}^{\text{start},G_{2,i,j}}$ values are supposed to be known at the beginning as the initial conditions.
2. Note that we have considered σ_c and τ_c to be constant for each driver w.r.t. time and space; therefore, we use σ_c and τ_c instead of $\sigma_{c,i,j}$ and $\tau_{c,i,j}$.
3. We consider a constant value for $v_{i,j}^{\text{free}}$ throughout the sampling road section $w_{i,j}$.

Disclosure statement

No potential conflict of interest was reported by the authors.

Funding

References

Bickel, P. J., C. Chen, J. Kwon, J. Rice, E. van Zwet, and P. Varaiya. 2007. "Measuring Traffic." *Statistical Science* 22 (4): 581–597.
Coifman, B. 2002. "Estimating Travel Times and Vehicle Trajectories on Freeways Using Dual Loop Detectors." *Transportation Research Part A* 36 (4): 351–364.
Daganzo, C. F. 1995. "The Cell Transmission Model, Part II: Network Traffic." *Transportation Research Part B: Methodological* 29 (2): 79–93.
Daganzo, C. F. 1997. *Fundamentals of Transportation and Traffic Operations.* Oxford: Pergamon-Elsevier.

Edie, L. C. 1963. "Discussion of Traffic Stream Measurements and Definitions." Proceedings of the 2nd international symposium on the theory of traffic flow, Paris, 139–154.

Han, J., J. W. Polak, J. Barria, and R. Krishnan. 2010. "On the Estimation of Space Mean Speed from Inductive Loop Detector Data." *Transportation Planning and Technology* 33 (1): 91–104.

Jamshidnejad, A., and B. De Schutter. 2015. "Estimation of the Generalized Average Traffic Speed Based on Microscopic Measurements." *Transportmetrica A: Transport Science* 11 (6): 525–546.

Kamijo, S., Y. Matsushita, K. Ikeuchi, and M. Sakauchi. 2000. "Traffic Monitoring and Accident Detection at Intersections." *IEEE Transactions on Intelligent Transportation Systems* 1 (2): 108–118.

Khisty, C. J., and B. K. Lall. 2003. *Transportation Engineering: An Introduction*. Upper Saddle River, NJ: Prentice Hall.

Klein, L. A., M. K. Mills, and D. R. Gibson. 2006. *Traffic Detector Handbook*. 3rd ed. Washington: US Department of Transportation, Federal Highway Administration.

Lee, C., B. Hellinga, and F. Saccomanno. 2006. "Evaluation of Variable Speed Limits to Improve Traffic Safety." *Transportation Research Part C: Emerging Technologies* 14 (3): 213–228.

Lighthill, M. J., and G. B. Whitham. 1955. "On Kinematic Waves. II. A Theory of Traffic Flow on Long Crowded Roads." *Proceedings of the Royal Society A: Mathematical, Physical and Engineering Sciences* 229 (1178): 317–345.

Messner, A., and M. Papageorgiou. 1990. "METANET: A Macroscopic Simulation Program for Motorway Networks." *Traffic Engineering and Control* 31 (9): 466–470.

Newell, G. F. 2002. "A Simplified Car-following Theory: A Lower Order Model." *Transportation Research Part B: Methodological* 36 (3): 195–205.

Rakha, H., and W. Zhang. 2005. "Estimating Traffic Stream Space Mean Speed and Reliability From Dual- and Single-loop Detectors." *Transportation Research Record* 1925: 38–47.

Sheu, J. B. 2002. "A Stochastic Optimal Control Approach to Real-time, Incident-responsive Traffic Signal Control at Isolated Intersections." *Transportation Science* 36 (4): 418–434.

Soriguera, F., and F. Robusté. 2011. "Estimation of Traffic Stream Space Mean Speed from Time Aggregations of Double Loop Detector Data." *Transportation Research Part C: Emerging Technologies* 19 (1): 115–129.

Treiber, M., and A. Kesting. 2013. *Traffic Flow Dynamics*. Berlin: Springer.

Wang, Y., M. Papageorgiou, and A. Messmer. 2006. "RENAISSANCE – A Unified Macroscopic Model-based Approach to Real-time Freeway Network Traffic Surveillance." *Transportation Research Part C: Emerging Technologies* 14 (3): 190–212.

Wardrop, J. G. 1952. "Road Paper. Some Theoretical Aspects of Road Traffic Research." *Proceedings of the Institution of Civil Engineers* 1: 325–362.